Clim. Past Discuss., doi:10.5194/cp-2015-184, 2016
Manuscript under review for journal Clim. Past
Published: 19 January 2016

Climate of the Past
Discussions
Open Access
EGU

Bering Sea surface water conditions during Marine Isotope Stages 12 to 10 at Navarin Canyon (IODP Site U1345)

Beth E. Caissie[1], Julie Brigham-Grette[2], Mea S. Cook[3], Elena Colmenero-Hidalgo[4]

[1]{Iowa State University, Ames, Iowa}

[2]{University of Massachusetts, Amherst, Amherst, Massachusetts}

[3]{Williams College, Williamstown, Massachusetts}

[4]{Universidad de León, León, Spain}

Correspondence to: B.E. Caissie (bethc@iastate.edu)

Abstract

Records of past warm periods are essential for understanding interglacial climate system dynamics. Marine Isotope Stage 11, occurred ~410 ka when global ice volume was the lowest, sea level was the highest and terrestrial temperatures were the warmest of the last 500 kyrs. This interval with its extreme character has been considered an analog for the near future. The Bering Sea is ideally situated to record how opening or closing the Pacific-Arctic Ocean gateway (Bering Strait) impacted primary productivity, sea ice, and sediment transport in the past; however, little is known about this region prior to 125 ka. IODP Expedition 323 to the Bering Sea offered the unparalleled opportunity to look in detail at time periods older than had been previously retrieved using gravity and piston cores. Here we present a multi-proxy record for Marine Isotope Stages 12-10 from Site U1345 located near the shelf-slope break. MIS 11 is bracketed by highly productive laminated intervals that may have been triggered by flooding of the Beringian shelf. Low insolation is associated with higher productivity, which was likely driven by increased upwelling. During the majority of MIS 11 however, high stratification appears to have

Clim. Past Discuss., doi:10.5194/cp-2015-184, 2016
Manuscript under review for journal Clim. Past
Published: 19 January 2016

led to lowered productivity in both the northern Atlantic and the northern Pacific. U1345, located near the marginal ice zone, experienced seasonal sea ice throughout both the glacial and interglacial stages. When global eustatic sea level was at its peak, Beringian tidewater glaciers advanced, driven by decreasing insolation, reduced seasonality, and high humidity due to high sea level and ice-free summers. Multiple examples of Pacific-Atlantic teleconnections are presented including laminations deposited at the end of MIS 11 in sync with millennial scale stadial events seen in the North Atlantic.

1 Introduction

Predictions and modeling of future climate change require a detailed understanding of how the climate system works. Reconstructions of previous warm intervals shed light on interhemispheric teleconnections. The most recent interglacial period when orbital conditions were similar to today was approximately 400 ka during the extremely long interglacial known as marine isotope stage (MIS) 11. Eccentricity was low, obliquity was high and the amplitude of precessional changes was low (Loutre and Berger, 2003). In addition, CO_2 concentration averaged approximately 275 ppm, which is similar to pre-industrial levels (EPICA community members, 2004). The transition from MIS 12 into MIS 11 has been compared to the last deglaciation (Dickson et al., 2009) and extreme warmth during MIS 11 has been considered an analog for future warmth (Droxler et al., 2003; Loutre and Berger, 2003), although the natural course of interglacial warmth today has been disrupted by anthropogenic forcing (IPCC, 2013).

Globally, MIS 11 is easily recognizable in the sediment record by an abrupt and distinct transition from high to low $\delta^{18}O$ values at the MIS 12/11 boundary and subsequent prolonged low values of $\delta^{18}O$ during MIS 11 (Lisiecki and Raymo, 2005). Furthermore, MIS 11 was unique in the polar regions. Antarctica experienced temperatures 2° C warmer than pre-industrial temperatures (Jouzel et al., 2007), and boreal forest extended across Greenland, which may have been largely ice free (de Vernal and Hillaire-Marcel, 2008). Large lakes in Siberia were anomalously productive and record warmer air and lake temperatures than today. Lake Baikal was 2° C warmer (Prokopenko et al., 2010) and Lake El'gygytgyn was 4° C warmer (Lozhkin and Anderson, 2013; Vogel et al.,

Clim. Past Discuss., doi:10.5194/cp-2015-184, 2016
Manuscript under review for journal Clim. Past
Published: 19 January 2016

2013). MIS 11 is also unique in Beringia because coastal glaciers advanced midway through the long interglacial cycle while sea level was still high (Brigham-Grette et al., 2001; Huston et al., 1990; Kaufman et al., 2001; Pushkar et al., 1999). This implies that parts of Beringia were glaciated rapidly as high latitude insolation fell in the northern hemisphere, but before global sea level dropped in response to the buildup of large ice sheets reaching lower latitudes. MIS 11 ice (i.e., leading to the Nome River Glaciation in MIS 10) is widely believed to be the last of the most extensive glaciations in central Beringia (Brigham-Grette et al., 2001; Gualtieri and Brigham-Grette, 2001; Kaufman et al., 1991; Manley et al., 2001).

Despite the work done to characterize the warmth of MIS 11 in the terrestrial realm (Candy et al., 2014; Melles et al., 2012; Prokopenko et al., 2010), as well as the North Atlantic (Bauch et al., 2000; Chaisson et al., 2002; Dickson et al., 2009; Milker et al., 2013; Poli et al., 2010), little is known about this interval from the Pacific region (Candy et al., 2014). Modeling studies describe several mechanisms for linking the Atlantic and Pacific through oceanic heat transport on glacial-interglacial scales (DeBoer and Nof, 2004; Hu et al., 2010), however, there have been no tests of these modeling studies using proxy data older than 30 ka. Furthermore, the location of the Bering Sea marginal ice zone advanced and retreated hundreds of kilometers during the past three glacial-interglacial cycles (Caissie et al., 2010; Katsuki and Takahashi, 2005; Sancetta and Robinson, 1983); however, sea surface and intermediate water variability before MIS 5 is unknown.

This investigation of terrestrial-marine coupling at the shelf-slope break from MIS 12 to 10 is the first study of this interval in the subarctic Pacific (Fig. 1). We use sedimentology, diatom assemblages, geochemistry, and calcareous nannofossil abundances as proxies for sea ice, sea surface conditions, and shelf to basin transport. These proxy records show changes in sea ice and glacial ice that are in sync with insolation changes at high northern latitudes. An interval of productivity occurs at the glacial termination (Termination V) that is both short-lived and intense. This is followed by evidence of glacial advance in Beringia during peak MIS 11 when sea level is high. We put these changes seen in the Bering Sea in the context of global records of MIS 11.

Clim. Past Discuss., doi:10.5194/cp-2015-184, 2016
Manuscript under review for journal Clim. Past
Published: 19 January 2016

Climate of the Past Discussions
Open Access
EGU

2 Background

2.1 Global Sea Level during MIS 11

The maximum height of sea level during MIS 11 is an open question with estimates ranging from more than 20 m above present sea level (apsl) (Kindler and Hearty, 2000) to 0 m apsl (Rohling et al., 2010). The discrepancy may stem from large differences between global eustatic (Bowen, 2010) or ice-volume averages (McManus et al., 2003) and regional geomorphological or micropaleontological evidence (van Hengstum et al., 2009). Regional isostatic adjustment due to glacial loading and unloading is also perhaps not as insignificant as previously assumed and regional highstands may record higher than expected sea levels if glacial isostasy and dynamic topography have not been accounted for, even in places that were never glaciated (Raymo and Mitrovica, 2012; Raymo et al., 2011). Work by Raymo and Mitrovica suggests that eustatic sea level during MIS 11 was 6-13 m apsl globally and near 5 m apsl locally in Beringia (Raymo and Mitrovica, 2012).

Regardless of the ultimate height of sea level, the transition from MIS 12 to MIS 11 was the greatest change in sea level of the last 500 ka (Rohling et al., 1998); sea level rose from -140 m to its present level or higher (Bowen, 2010). Up to three highstands occurred during MIS 11 (Kindler and Hearty, 2000), the highest at the second June insolation peak at 65°N. This highstand is referred to as MIS 11.3 and occurs 406 ka (Bassinot et al., 1994). Sea levels above modern require partial or complete collapse of the Greenland ice sheet (up to 6 m) (de Vernal and Hillaire-Marcel, 2008) and/or the West Antarctic Ice Sheet (Scherer et al., 1998), but not the East Antarctic Ice Sheet (Berger et al., 2015; Raymo and Mitrovica, 2012). It has frequently been hypothesized that the West Antarctic Ice Sheet collapsed during MIS 11 and modeling studies confirm this (Pollard and DeConto, 2009), however drilling in Antarctica was not able to confirm a collapse (Naish et al., 2009). East Antarctica appears stable; however, small changes in either Antarctic ice sheet may have contributed up to 5 m of sea level rise (Berger et al., 2015; EPICA community members, 2004).

Clim. Past Discuss., doi:10.5194/cp-2015-184, 2016
Manuscript under review for journal Clim. Past
Published: 19 January 2016

2.2 Sea Level Variation in Beringia

Beringia refers to both the terrestrial and marine regions north of the Aleutian Islands that stretch to the shelf-slope break in the East Siberian, Chukchi, and Beaufort seas (Fig. 1). On land, Beringia extends from the Lena River in Siberia to the Mackenzie River in Canada. Large portions of the Beringian shelf are exposed when sea level drops below -50 m (Hopkins, 1959) and this subaerial expanse stretches more than 1000 km from north to south during glacial periods (Fig. 2). In contrast, as sea level rises at glacial terminations the expansive continental shelf is flooded, introducing fresh organic matter and nutrients into the southern Bering Sea (i.e. Bertrand et al., 2000; Ternois et al., 2001) and re-establishing the connection between the Pacific and Atlantic oceans through Bering Strait.

2.3 Beringian Hydrography

Today, water circulates cyclonically in the deep basins of the Bering Sea (Fig. 1). Site U1345 is influenced by the northwest flowing Bering Slope Current, which is derived from the Alaskan Stream. South of the Aleutians Islands, the Alaskan Stream flows westward and enters the Bering Sea through deep channels in the western Aleutian Islands. Once north of the Aleutian Islands, this water mass is called the Aleutian North Slope Current, and flows eastward until it reaches the Bering Sea shelf. Interactions with the shelf turn this current to the northwest where it becomes the Bering Slope Current (Stabeno et al., 1999). Tidal forces and eddies in the Bering Slope Current drive upwelling through Navarin Canyon and other interfluves along the shelf-slope break (Kowalik, 1999). The resulting cold water and nutrients brought to the sea surface, coupled with the presence of seasonal sea ice, drive the high productivity found today in the so called “Green Belt” (Springer et al., 1996) along the shelf-slope break. North of the site, low salinity, high nutrient shelf waters (Cooper et al., 1997) primarily flow north through the Bering Strait to the Arctic Basin (Schumacher and Stabeno, 1998).

Major changes in circulation may have occurred throughout MIS 12 to 10 due to sea level rise and fall, the strength of North Atlantic Deep Water (NADW) formation, and the intensity of winds originating in the Southern Ocean (e.g. DeBoer and Nof, 2004; Hu et

Clim. Past Discuss., doi:10.5194/cp-2015-184, 2016
Manuscript under review for journal Clim. Past
Published: 19 January 2016

al., 2010). Specifically, as sea level rose after MIS 12, the connection between the Pacific and the Atlantic was reestablished. De Boer and Nof (2004) suggest that under high sea level conditions, if freshwater is suddenly released into the North Atlantic, the Bering Strait might act as an "exhaust valve" allowing fresh water from the North Atlantic to flow into the Arctic Ocean and then flow south through the Bering Strait, thus preventing a shut-down in thermohaline circulation (DeBoer and Nof, 2004). Hu et al. (2010) suggest that when sea level is fluctuating near the sill depth of Bering Strait (~ -50 m apsl today), this gateway can modulate widespread climate changes. When Bering Strait is open and North Pacific water is transported to the North Atlantic, the less saline Pacific water can freshen the North Atlantic and slow meridional overturning, subsequently cooling the North Atlantic, but warming the North Pacific. This North Atlantic cooling can result in the buildup of ice sheets and global sea level drops, closing Bering Strait. A closed Bering Strait concentrates fresher waters in the North Pacific and more saline waters in the North Atlantic. A more saline Atlantic means that stratification is low and meridional overturning is increased. This increases oceanic heat transport to the North Atlantic, triggers warming in the North Atlantic and ultimately ice sheets retreat and sea level rises reconnecting the Pacific with the Atlantic (Hu et al., 2010).

3 Methods

3.1 Study Area and Sampling

The Integrated Ocean Drilling Program's (IODP) Expedition 323, Site U1345, is located on an interfluve ridge near the shelf-slope break in the Bering Sea (Fig. 1). Navarin Canyon, one of the largest submarine canyons in the world (Normack and Carlson, 2003) is located just to the northwest of the site. Sediments were retrieved from ~1008 m of water, placing the site within the center of the modern day oxygen minimum zone (Takahashi et al., 2011). We focus on this site because of its proximity to the modern marginal ice zone in the Bering Sea and observed high sedimentation rates.

Site U1345 was drilled five times during Exp. 323 and cores from four of these holes were described onboard the JOIDES Resolution. This study focuses on a splice of 3 holes that were correlated onboard the ship, so that core gaps in one hole are covered by core

Clim. Past Discuss., doi:10.5194/cp-2015-184, 2016
Manuscript under review for journal Clim. Past
Published: 19 January 2016

material in other holes. In addition to the original analyses presented here, we refer to the shipboard core descriptions and physical properties data (Takahashi et al., 2011) in our interpretations. Depths are reported in CCSF-A, a correlated depth scale that allows for direct comparison between drill holes. Units are meters below sea floor (mbsf). A small syringe was used to collect approximately 1 cc of sediment periodically between 112.96 m and 136.40 mbsf. Sampling resolution varied for each analysis. Hyalochaete *Chaetoceros* resting spores were counted on average every 20 cm (~600 yr resolution), full diatom counts were carried out every 36 cm (~1000 yr resolution), calcareous nannofossils were counted every 40 cm (~1200 yr resolution), grain size was analyzed every 23 cm (670 yr resolution), and geochemistry was analyzed every 30 cm (800 yr resolution).

3.2 Age Model

The age model (Fig. 3) is derived from the shipboard age model, which was developed using magnetostratigraphy and biostratigraphy. First and last appearance datums for diatoms and radiolarians make up the majority of the biostratigraphic markers used to place the record in the correct general stratigraphic position (Takahashi et al., 2011). Oxygen isotope measurements taken on the benthic foraminifera, *Uvigerina peregrina, Nonionella labradorica, and Globobulimina affinis* (Cook et al., In Press) were then used to tune site U1345 to the global marine benthic foraminiferal isotope stack (LR04) (Lisiecki and Raymo, 2005) (Fig. 3). Based on this combined age model, MIS 11 spans from 115.3 to 130.6 mbsf (Cook et al., In Press); however, the characteristic interglacial isotopic depletion was not found in U1345 which means that the exact timing of peak interglacial conditions is unknown.

The nearby core, IODP Exp 323, Site U1343 (Fig. 1) has an excellent oxygen isotopic record during MIS 11 (Kim et al., 2014). We compared the two isotopic records and their magnetic susceptibilities (Fig. 3) and found that even with only two tie points, there was good correlation between the timing of the onset of laminated intervals and also the interglacial increase in magnetic susceptibility (Fig. 3). We added one additional tie point to connect the inflection points in magnetic susceptibility. In U1343, this point occurred

Clim. Past Discuss., doi:10.5194/cp-2015-184, 2016
Manuscript under review for journal Clim. Past
Published: 19 January 2016

at 398.50 ka. U1345 was shifted 1.5 ka younger in order to align with U1343. The addition of this point allows us to have more confidence in the timing of peak interglacial conditions in U1345. However, given the oxygen isotope sampling resolution, as well as the stated error in the LR04 dataset (4 kyr), we estimate the error of the age model could be up to 5 kyr. Therefore, we urge caution when interpreting millennial scale changes at the site or comparing our record to others that examine MIS 11 at millennial scale resolution or finer.

Sedimentation rates during the study interval range from 29 cm/kyrs to 45 cm/kyr with the highest sedimentation rates occurring during glacial periods.

3.3 Diatom Analysis

In order to quantify the number of diatom valves deposited per gram of sediment, diatom slides were prepared according to the method described in Scherer (1994). This method allows for a direct comparison of diatom accumulation in the sediments between samples, though not diatom flux. Cover slips were mounted on cleaned microscope slides using hyrax in toulene (refractive index: 1.7135). At least 300 diatom valves were identified in at least three random transects across the slide using a light microscope at magnifications from 1000x to 1250x (see Armand et al., 2005; Sancetta, 1979; Sancetta and Silvestri, 1986; Scherer, 1994). The portion of the slide that was examined was measured using a stage micrometer. Partial valves were counted according to the methods of Schrader and Gersonde (1978). All diatoms were identified to the species level when possible following published taxonomic descriptions and images (Hasle and Heimdal, 1968; Koizumi, 1973; Lundholm and Hasle, 2008, 2010; Medlin and Hasle, 1990; Medlin and Priddle, 1990; Onodera and Takahashi, 2007; Sancetta, 1982, 1987; Syvertsen, 1979; Tomas, 1996; Witkowski et al., 2000). Diatom counts were transformed into relative percent abundances. Absolute abundances (diatoms per gram sediment) were calculated following the methods of Scherer (1994). Diatom taxa were then grouped according to ecological niche (Table 1) based on biological observations (Aizawa et al., 2005; Fryxell and Hasle, 1972; Håkansson, 2002; Horner, 1985; Saito and Taniguchi, 1978; Schandelmeier and Alexander, 1981; von Quillfeldt, 2001; von Quillfeldt et al., 2003)

Clim. Past Discuss., doi:10.5194/cp-2015-184, 2016
Manuscript under review for journal Clim. Past
Published: 19 January 2016

and statistical associations (Barron et al., 2009; Caissie et al., 2010; Hay et al., 2007; Katsuki and Takahashi, 2005; Lopes et al., 2006; McQuoid and Hobson, 2001; Sancetta, 1982, 1981; Sancetta and Robinson, 1983; Sancetta and Silvestri, 1986; Shiga and Koizumi, 2000). In cases where a diatom species was reported to fit into more than one environmental niche, it was grouped into the niche where it was most commonly recognized in the literature.

3.4 Calcareous Nannofossils

In order to quantify calcareous nannofossils per gram of sediment, a total of 18 samples were prepared following the methodology of Flores and Sierro (1997). A known mass of dried sediment was diluted in a known volume of buffered water. A small fraction was extracted with a micropipette and dropped onto a petri dish previously filled with buffered water and with a cover slip in its bottom. After settling overnight, the excess water was removed and the slide was left to dry and then mounted using Canada balsam.

Observations were made using a Zeiss polarized light microscope at 1000x magnification. Samples were considered barren if no coccoliths were found in at least 165 randomly selected fields of view. All taxa were identified to the species or variety level, following Flores et al. (1999) and Young et al. (2003).

3.5 Grain Size

Volume percent of grains in 109 size bins ranging from 0.01 μm to 3500 μm was measured using a Malvern Mastersizer 3000 with the Hydro MV automated wet dispersion unit. Samples were prepared by adding 200 μl of the deflocculant, sodium hexametaphosphate, to 0.2 mg dry sediment. In this way, we were able to quantify all sediment types including biogenic and terrigenous grains.

Clim. Past Discuss., doi:10.5194/cp-2015-184, 2016
Manuscript under review for journal Clim. Past
Published: 19 January 2016

3.6 Geochemistry

Sediment samples were freeze-dried then ground. An aliquot of homogenized sediment was treated to remove carbonates using pH 5 buffered acetic acid. The carbon (from the acidified sediment) and nitrogen (from the unacidified sediment) isotopic and elemental composition of organic matter was determined by Dumas combustion using a Carlo Erba 1108 elemental analyzer coupled to a Thermo-Finnigan Delta Plus XP isotope ratio mass spectrometer at the University of California Santa Cruz Stable Isotope Laboratory. The 1-sigma precision of stable isotope measurements and elemental composition of carbon are 0.2‰ and 0.03%, respectively, and for nitrogen are 0.2‰ and 0.002%, respectively. Percent $CaCO_3$ was calculated according to Schubert and Calvert (2001).

4 Results

4.1 Sedimentology

In general the sediments at Site U1345 are massive with centimeter–scale dark or coarse-grained mottles. The sediments are mainly composed of clay and silt with varying amounts of diatoms, sand, and tephra throughout. Laminated intervals bracket MIS 11 (Fig. 4). The proportion of diatoms relative to terrigenous or volcanogenic grains is highest during laminated intervals and lowest immediately preceding Termination V (~425 ka). Vesiculated tephra shards were seen in every diatom slide analyzed. Several thin (< 1 cm) sand layers and shell fragments were visible on the split cores, especially during MIS 12. However, high-resolution grain size analyses show that the median grain size was lowest during MIS 12, increasing from approximately 14 μm to 21 μm at the start of Termination V at 424.5 ka (130.92 mbsf). Median grain size peaks at 84 μm between 401 and 407 ka (125.42-123.62 mbsf). This interval is also the location of an obvious sandy layer in the core. After this interval, median grain size remains steady at about 17 μm. Subrounded to rounded clasts (granule to pebble) commonly occur on the split surface of the cores. We combined clast and sand layer data from all Holes at Site U1345 when examining their distribution (Fig. 4).

Clim. Past Discuss., doi:10.5194/cp-2015-184, 2016
Manuscript under review for journal Clim. Past
Published: 19 January 2016

292 A 3.5 m thick laminated interval, estimated to span 12 kyrs (see Table 2 for depths and
293 ages) is deposited beginning during Termination V. Although the termination is short
294 lived and the laminated interval quite long, we refer to it as the Termination V
295 Laminations for the sake of clarity throughout this manuscript. The next laminated
296 interval occurs at about 394 ka and lasts approximately 1100 years. During the transition
297 from late MIS 11 to MIS 10, a series of four thin laminated intervals are observed. Each
298 interval lasts between 0.34 and 1.25 ka (Table 2). In general, the upper and lower
299 boundaries of laminated intervals are gradational; however the boundaries between
300 individual lamina are sharp (Takahashi et al., 2011). There are two types of laminations.
301 The Termination V Laminations are Type I laminations: millimeter-scale alternations of
302 black, olive gray, and light brown triplets. In addition to containing a high proportion of
303 diatoms, this laminated interval also contains high relative proportions of calcareous
304 nannofossils and foraminifera (Takahashi et al., 2011). The majority of laminations are
305 parallel; however, a 7 cm interval during the Termination V Laminations is highly
306 disturbed in Hole A, showing recumbent folds in the laminations (Takahashi et al., 2011).
307 This interval was not sampled. Type II laminations occur throughout the remainder of
308 MIS 11. These laminations have fewer diatoms and tend to be couplets of siliciclastic
309 sediments with <40% diatoms (Takahashi et al., 2011). Percent $CaCO_3$ also increases
310 during these laminations though foraminifera and calcareous nannofossils are very rarely
311 seen. None of these later laminated intervals contain any evidence of disturbance.

312

313 ## 4.2 Diatoms

314 ### 4.2.1 Diatom Assemblages

315 A total of 97 different diatom taxa were identified. Individual samples include between
316 26 and 46 taxa each with an average of 37 taxa. Both types of laminated intervals contain
317 fewer taxa than bioturbated intervals do. This decrease in diversity is confirmed using the
318 Margalef, Simpson, and Shannon indices which all show similar down-core profiles (Fig.
319 5). The Margalef index is a measure of species richness (Maurer and McGill, 2011). It
320 shows a decrease in the number of taxa during four out of five laminated intervals that are
321 sufficiently well sampled. Between laminated intervals, there is a noted decrease in taxa

Clim. Past Discuss., doi:10.5194/cp-2015-184, 2016
Manuscript under review for journal Clim. Past
Published: 19 January 2016

at 388 ka. Instead of species richness, the Simpson index measures the evenness of the sample. Values close to 1 indicate that all taxa contain an equal number of individuals, while values close to 0 indicate that one species dominates the assemblage (Maurer and McGill, 2011). In general, the Simpson index is close to 1 throughout the core indicating a rather even distribution of diatom valves across all taxa; however, during the Termination V Laminations and the most recent two laminations, the Simpson index drops reflecting the dominance by *Chaetoceros* RS during these intervals (Fig. 5). It does not come close to 0, which would likely indicate a strong dissolution signal. The Shannon diversity index measures both species richness and evenness (Maurer and McGill, 2011). Correspondingly, it is low during three of the laminated intervals, high during MIS 12 and peaks at 397 ka (Fig. 5).

Absolute diatom abundances vary between 10^6 and 10^8 diatoms deposited per gram of sediment with values an order of magnitude higher during most laminated intervals than during massive intervals (Fig. 5). The diatom assemblage is dominated by *Chaetoceros* and *Thalassiosira antarctica* resting spores (RS), with lesser contributions from *Fragilariopsis oceanica, Fragilariopsis cylindrus, Fossula arctica, Shionodiscus trifultus* (=*Thalassiosira trifulta), Thalassiosira binata,* small (<10 µm in diameter) *Thalassiosira* species, *Paralia sulcata, Lindavia* cf. *ocellata*, *Neodenticula seminae,* and *Thalassionema nitzschioides,* (Fig. 6).

Relative percent abundances of *Chaetoceros* RS are highest (up to 69%) during the Termination V Laminations and, in general, mimic the pattern of both diatom accumulation rate and insolation at 65° N (Berger and Loutre, 1991). When insolation is low, *Chaetoceros* RS are also low (Fig. 7). *T. antarctica* RS, in contrast, are lowest during the Termination V Laminations (as low at 1%) and higher during MIS 12 and after 406 ka (above 125.00 mbsf and 112.97 mbsf). This taxon peaks at 38% relative abundance at 390 ka (120.45 mbsf; Fig. 6).

Relative percent abundances of the characteristic marginal ice zone species, *F. oceanica* and *F. cylindrus* (Caissie et al., 2010; Saito and Taniguchi, 1978; Sancetta, 1982; von Quillfeldt et al., 2003), oscillate between ~10% and less than 3% of the diatom assemblage and are highest during MIS 12 and all laminated intervals. They are both at

Clim. Past Discuss., doi:10.5194/cp-2015-184, 2016
Manuscript under review for journal Clim. Past
Published: 19 January 2016

their lowest between ~411 to ~400 ka (126.62 to 123.45 mbsf). The neritic species and moving water indicator, *P. sulcata* is lowest during the laminated intervals. It reaches a maximum (34% relative abundance) at 404 ka (124.61 mbsf). *P. sulcata* remains moderately high (~10%) during non-laminated intervals. *L.* cf. *ocellata* is the dominant taxa in the fresh water group and the variability in its abundances is discussed below. *S. trifultus* follows a very similar distribution to the fresh water group and *L.* cf. *ocellata*. It is relatively high (~4%) during MIS 12, is virtually absent from the sediments during the Termination V Laminations, and then increases again until it peaks at 10% relative abundance at 400 ka (123.22 mbsf). *Thalassiosira binata* and other small (<10 µm in diameter) *Thalassiosira* species have similar distributions with low relative abundances throughout the record (< 6%) except for a small peak between 397 and 386 ka (122.62 and 119.07 mbsf. The relative percent abundances of *N. seminae* are discussed below. The largest peak in *N. seminae* is at 392 ka (121.2 mbsf) (Fig. 6).

4.2.2 Diatom Proxies

Diatoms, like many organisms, thrive under a specific range of environmental conditions or optima and these optima are different for each species. For this reason, diatom assemblages are excellent paleoceanographic indicators (Smol, 2002). Table 1 delineates which species were grouped together into specific environmental niches. Our interpretations of the paleoceanographic sea surface conditions at the Bering Sea shelf-slope break during MIS 12 to 10 are based on changes in these 8 groups and the variability of *Neodenticula seminae*, an indicator of the Alaskan Stream and North Pacific water (Katsuki and Takahashi, 2005; Sancetta, 1982) (Fig. 7).

4.2.2.1 Sea Ice Species

Epontic diatoms are those that bloom attached to the underside of sea ice or within brine channels in the ice. This initial bloom occurs below the ice as soon as enough light penetrates to initiate photosynthesis in the Bering Sea, which can occur as early as March (Alexander and Chapman, 1981). The centric diatom, *Melosira arctica,* and pennate

Clim. Past Discuss., doi:10.5194/cp-2015-184, 2016
Manuscript under review for journal Clim. Past
Published: 19 January 2016

diatoms, *Nitzschia frigida* and *Navicula transitrans* are among the major components of the epontic diatom bloom (von Quillfeldt et al., 2003) and all are found in the sediments at U1345A, although they tend to be quite rare.

A second ice-associated bloom occurs as sea ice begins to break up on the Bering Sea shelf. This bloom is referred to as the marginal ice zone bloom and many of its members are common species in the sediment assemblage including the pennate diatom, *Staurosirella* cf. *pinnata* (=*Fragilaria* cf. *pinnata*), and the centric diatoms, *Bacterosira bathyomphala* and several *Thalassiosira* species including *Thalassiosira antarctica* (Schandelmeier and Alexander, 1981; Shiga and Koizumi, 2000; von Quillfeldt et al., 2003). *T. antarctica* resting spores have been classified in various ways in the past and their ecology is not well understood. However, *T. antarctica* is a member of the marginal ice zone flora (von Quillfeldt et al., 2003) and was the only organism found in thick pack ice (Horner, 1985). The resting spores are associated with coastal or ice-margin waters that range from −1 to 4° C and have relatively low salinity (25–34‰) (Barron et al., 2009; Shiga and Koizumi, 2000). In Antarctica, *T. antarctica* blooms in concert with frazil and platelet ice growth in the fall (Pike et al., 2009). This same association has not yet been observed in the Arctic, though it is a possibility. High abundances might indicate that ice formed early enough in the fall that light and/or nutrients were high enough to support *T. antarctica* growth then.

Several diatom species are present in both types of sea ice blooms, and so while they are indicators of ice presence, they cannot be used to distinguish between types of sea ice. These species are grouped under “both ice types” and include such common diatoms as *Fragilariopsis oceanica, Fragilariopsis cylindrus, Fossula arctica,* and many Naviculoid pennate diatoms (Saito and Taniguchi, 1978; Sancetta, 1981; Schandelmeier and Alexander, 1981; von Quillfeldt, 2001; von Quillfeldt et al., 2003).

Epontic species are present in low relative percent abundances (< 5%) throughout much of the record, but there is a marked absence of them during the laminated interval from 423 to 410 ka (129.96-126.45 mbsf). Marginal ice zone species fluctuate between 4% and 14% throughout the record and do not show any trends in abundance changes. The

Clim. Past Discuss., doi:10.5194/cp-2015-184, 2016
Manuscript under review for journal Clim. Past
Published: 19 January 2016

grouping of species found both within the ice and in the water surrounding ice, however, is also somewhat reduced during laminated intervals (Fig. 7).

4.2.2.2 Warmer Water Species

Diatoms associated with warmer water or classified as members of temperate to subtropical assemblages are rare in this record; however, they are present. This group includes *Azpeitia tabularis, Thalassiosira eccentrica, Shionodiscus oestrupii* (=*Thalassiosira oestrupii*), and *Thalassiosira symmetrica.* (Fryxell and Hasle, 1972; Lopes et al.; Sancetta; Sancetta and Silvestri, 1986).

Relative abundances of warmer water species are quite low throughout the record (<5%), and are highest (3-4%) during mid to late MIS 11 approximately ~410 to 391 ka (126.74 to 116.50 mbsf) (Fig. 7).

4.2.2.3 Alaskan Stream Species

Neodenticula seminae is often used as a tracer of North Pacific water, in particular the Alaskan Stream (e.g. Caissie et al., 2010; Katsuki and Takahashi, 2005). But its distribution also varies on glacial-interglacial time scales within the Pacific Ocean (Sancetta and Silvestri, 1984). It is adapted to the low productivity of the North Pacific gyre and is heavily silicified which could lead to high proportions of *N. seminae* reflecting simply dissolution of finely silicified diatoms (Sancetta, 1982, 1981). *N. seminae* is used here as a tracer of Pacific water with the above caveats.

Absolute abundances of *N. seminae* began to increase at 422 ka as global eustatic sea level rises above -50 mapsl. Abundance then decreases slowly over the course of the Termination V Laminations and peaks again at 392 ka and 382 ka. As sea level drops below -50 mapsl, *N. seminae* is no longer present at U1345. Relative percent abundances remain stable at ~2% relative percent abundance between 422 and 400 ka (129.62-123.62 mbsf), then peaks at 13% at 392 ka (121.22 mbsf) (Fig. 6). Low proportions of *N. seminae* during the Termination V Laminations are likely due to the overwhelming proportion of *Chaetoceros* RS during this time.

Clim. Past Discuss., doi:10.5194/cp-2015-184, 2016
Manuscript under review for journal Clim. Past
Published: 19 January 2016

4.2.2.4 High Productivity Species

Chaetoceros resting spores are the dominant taxa included in the high productivity group. *Chaetoceros* RS have been used as indicators of high productivity (e.g. Caissie et al., 2010) and are often found in locations influenced by intense upwelling (Lopes et al., 2006; Sancetta, 1982). In addition, *Chaetoceros socialis* can be a common member of the marginal ice zone bloom (von Quillfeldt, 2001) and a dominant member of the sub ice bloom (Melnikov et al., 2002). *Chaetoceros furcellatus* is also associated with the marginal ice zone bloom (von Quillfeldt, 2001). Unfortunately, the morphology of *Chaetoceros* resting spores is quite variable, and they cannot be classified definitively without the more labile vegetative cell also present (Tomas, 1996). *Odontella aurita, Thalassionema nitzschioides* are also included in the high productivity group although they are also associated with the marginal ice zone (von Quillfeldt et al., 2003), areas of high productivity (Aizawa et al., 2005), and upwelling (Lopes et al., 2006; Sancetta, 1982). It should be noted that we can not discern between high productivity due to upwelling and high productivity due to other factors because the diatom proxies are not sufficiently refined to distinguish between the two.

It may be that the combination of upwelling and ice melt at the shelf slope break in the Bering Sea is responsible for correlation between these two environmental niches. The spring-blooming *Thalassiosira pacifica* and small (<10 μm) *Thalassiosira* species round out the high productivity group due to their associations with high productivity and upwelling specifically in the Bering Sea and North Pacific (Aizawa et al., 2005; Hay et al., 2007; Katsuki and Takahashi, 2005; Lopes et al., 2006; McQuoid and Hobson, 2001; Saito and Taniguchi, 1978).

Like *Chaetoceros* RS, high productivity species mimic the trend of the insolation curve (Berger and Loutre, 1991) with highest relative abundances (60-70%) occurring during high levels of insolation (Fig. 7). The lowest relative abundances (15-20%) of high productivity species occur between 403 and 390 ka (124.21 to 120.07 mbsf) when both obliquity and insolation are low. High productivity species are high during both the Termination V Laminations and during the late MIS 11 laminations (Fig. 7).

Clim. Past Discuss., doi:10.5194/cp-2015-184, 2016
Manuscript under review for journal Clim. Past
Published: 19 January 2016

Climate of the Past Discussions
Open Access
EGU

469

470 4.2.2.5 Dicothermal Water Indicators and Late Summer Species

471 A cold layer of water found between seasonally warmer surface and warmer deep water
472 characterizes dicothermal water. It is stable because of its very low salinity. In the Sea of
473 Okhotsk and the Bering Sea, the dicothermal layer is often associated with melting sea
474 ice. The highest abundances of *Shionodiscus trifultus* are found associated with this
475 highly stratified, cold water in the Sea of Okhotsk today (Sancetta, 1981; Sancetta and
476 Silvestri, 1986).

477 *Actinocyclus curvatulus* has been observed living in water surrounding sea ice (von
478 Quillfeldt et al., 2003); however, it is neither a common member of the marginal ice zone
479 flora, nor is its spatial distribution in the Bering Sea consistent with the distribution of sea
480 ice (Sancetta, 1982). Its relative percent abundances are more closely associated with
481 those of *S. trifultus* (Sancetta, 1982), and so it was grouped with *S. trifultus* as an
482 indicator of dicothermal water.

483 Genera present in the Bering Sea during late summer (*Coscinodiscus, Leptocylindrus,*
484 and *Rhizosolenia*) (Aizawa et al., 2005; Lopes et al., 2006; von Quillfeldt et al., 2003)
485 tend to co-vary with the dicothermal water indicators, so the two groups were merged for
486 comparison with other diatom groups.

487 These two groups are highest (18% relative abundance) at ~401 ka (123.62 mbsf) as
488 insolation declines. This peak is coeval with the peak in fresh water species and an
489 intermediate peak in *N. seminae* and occurs immediately following a peak in neritic
490 species. Dicothermal water indicators and summer species are lowest (< 1%) during the
491 Termination V Laminations (~424-412 ka). Intermediate relative abundances (1% to 5%)
492 occur during MIS 12 and above 392 ka (121.04 mbsf) (Fig. 7).

493

494 4.2.2.6 Shelf to Basin Transport Indicators

495 Freshwater species are rare, but present in the record. They include the centric species
496 *Lindavia* cf. *ocellata* and *L. radiosa* (Håkansson, 2002). Additional freshwater diatoms
497 found in the record are species also found in sea ice (*S.* cf. *pinnata*) (von Quillfeldt et al.,

Clim. Past Discuss., doi:10.5194/cp-2015-184, 2016
Manuscript under review for journal Clim. Past
Published: 19 January 2016

2003) or in the neritic zone (*Cyclotella stylorum)* (Barron et al., 2009) and so these species were placed in the marginal ice zone and neritic groups respectively.

The dominant species in the neritic group is *Paralia sulcata,* which is an interesting species because it can be either planktic or benthic (Kariya et al., 2010) and is associated both with river deltas and the species *Melosira sol* (Sancetta, 1982). It can be a member of the marginal ice zone assemblage (von Quillfeldt et al., 2003) though Pushkar (1999) asserts that *P. sulcata* indicates water shallower than 20 m. Its high abundances in Bering Strait may mean that it is adapted to moving water (Sancetta, 1982). *P. sulcata* thrives in water that is warmer than 3 degrees (Zong, 1997), with low light (Blasco et al., 1980) and low salinity (Ryu et al., 2008).

The fresh water group is notably absent from much of the core, but prevalent between 401 and 392 ka (123.70 mbsf and 121.20 mbsf); it reaches its highest relative percent abundance (12%) at 401 ka (123.62 mbsf). Neritic species, on the other hand maintain ~10% relative abundance throughout the core. They are lowest during the Termination V Laminations and increase dramatically around 404 ka (124.61 mbsf) to almost 50% of the assemblage (Fig. 7).

4.3 Calcareous Nannofossils

Calcareous nannofossils were examined between 432-405 ka (133.4 to 125.0 mbsf); one third of the samples were barren and only one sample (418 ka; 128.8 mbsf) had sufficient individuals to estimate relative percent abundances (Fig. 7). This sample is located midway through the Termination V Laminations when the diatom assemblage is overwhelmingly dominated by *Chaetoceros* RS. Small *Gephyrocapsa* dominates (>50%) the calcareous nannofossil assemblage. There are 35% medium *Gephyrocapsa,* 9% *Coccolithus pelagicus*, and 1% *G. oceanica*.

Clim. Past Discuss., doi:10.5194/cp-2015-184, 2016
Manuscript under review for journal Clim. Past
Published: 19 January 2016

4.4 Geochemistry

4.4.1 Organic and Inorganic Carbon Content

Total organic carbon (TOC) roughly follows the trend of relative percent abundances of *Chaetoceros* RS, with higher values during the Termination V Laminations. Mean TOC value during MIS 12 is 0.76%, and during the Termination V Laminations, it is 1.11%. TOC decreases temporarily in sync with depleted $\delta^{15}N$ values, before rising linearly from 404 ka (124.77 mbsf) to 374 ka (115.39 mbsf). TOC is again high during the late MIS 11/MIS 10 laminations.

In contrast, inorganic carbon, calculated as % $CaCO_2$ is less than 1% for most of the record; however, it increases up to 3.5% during the laminated intervals and also at 382 ka (117.87 mbsf), 392 ka (110.00 mbsf), and 408 ka (125.82 mbsf).

4.4.2 Terrigenous Input Indicator (C/N)

The ratio, C/N is one of two proxies used as indicators of marine versus terrigenous organic matter, with marine values typically ranging from 5-7 and terrigenous ratios over 20 (Meyers, 1994; Redfield et al., 1963).

Throughout the record, C/N indicates primarily a marine source for organic matter. During MIS 12, C/N is highly variable, when sea level is below -50 m apsl. As sea level rises during Termination V, C/N values increase from 6 to more than 9. The highest C/N value occurs at the start of the Termination V Laminations. C/N decreases as sea level rises until at 400 ka (123.62 mbsf) it stabilizes near 7 for the remainder of the record.

4.4.3 Bulk Sedimentary Stable Isotopes

4.4.3.1 Carbon Isotopes

Stable isotopes of carbon are also used as an indicator of marine vs. terrigenous organic matter with $\delta^{13}C$ values near -27 indicating C3 plant-sourced organic matter; values between -22 and -19 are typical for Arctic Ocean marine phytoplankton and -18.3 is average for ice-related plankton (Schubert and Calvert, 2001). However, it has been

Clim. Past Discuss., doi:10.5194/cp-2015-184, 2016
Manuscript under review for journal Clim. Past
Published: 19 January 2016

shown that $\delta^{13}C$ is sometimes related more to growth rate, cell size, and cell membrane permeability, so it may reflect changing phytoplankton groups instead of simply marine vs. C3 plant sources of organic matter in U1345.

Carbon isotopic values range between -22 ‰ and -26 ‰ and are generally anticorrelated with C/N values. These values indicate a mix of marine phytoplankton and C3 plants as the main contributors to organic matter at the site. At the onset of the Termination V Laminations, $\delta^{13}C$ becomes more negative and then gradually increases to a maximum of -22.33 at 404 ka (124.62). After 400 ka (123.5 mbsf), $\delta^{13}C$ is relatively stable around -23.5‰.

4.4.3.2 Nitrogen Isotopes

Nitrogen, in the form of nitrate, is a key nutrient for phytoplankton growth. Diatoms preferentially assimilate the lighter isotope, ^{14}N, which in turn enriches surface waters with respect to ^{15}N (Barron et al., 2009; Shiga and Koizumi, 2000). Keeping in mind the effects of nitrification of oxygen rich and poor sediments (Brunelle et al., 2007), the efficiency of nitrogen utilization can be estimated by examining the $^{15}N/^{14}N$ ratio of nitrogen in either bulk sedimentary organic matter, with enriched values of $\delta^{15}N$ indicating higher nutrient utilization. Sponge spicules (very low $\delta^{15}N$ values) and radiolarians (highly variable $\delta^{15}N$ values) may contaminate the $\delta^{15}N$ of bulk organic matter, however we looked for and found no correlation between spicule abundance and $\delta^{15}N$ in our samples.

Surprisingly, $\delta^{15}N$ is relatively stable throughout the study interval, fluctuating around an average value of 6.4‰, though there are several notable excursions. Coeval with sea level rise and increased relative percent *Chaetoceros* RS, $\delta^{15}N$ decreased 2.7‰ to 4.4‰ before recovering to average values during the Termination V Laminations. Two other depletions occur at 405 ka (124.77 mbsf) and 393 ka (121.62 mbsf), the first is the most extreme and reaches 2.9‰.

Clim. Past Discuss., doi:10.5194/cp-2015-184, 2016
Manuscript under review for journal Clim. Past
Published: 19 January 2016

5 Discussion

The study interval can be broken into five zones based on changes in diatom assemblages and lithology (Fig. 7): MIS 12, Termination V, Peak MIS 11, Beringian Glacial Initiation, and Late MIS 11. These zones reflect changing sea ice, glacial ice, sea level, and SST and correspond to events recognized elsewhere in ice cores and marine and lake sediments.

5.1 Marine Isotope Stage 12 and Early Deglaciation (beginning of record to 425 ka)

The beginning of the record to 425 ka chronicles conditions at the end of MIS 12. Although diatom accumulation rate is quite low, a relatively diverse assemblage characterizes this period (Fig. 5) with moderate amounts of sea ice, high productivity, and dicothermal species (Fig. 7), indicating seasonal sea ice with highly stratified waters during the ice-melt season. Nitrogen isotopes indicate high nutrient utilization (Fig. 7) consistent with nitrogen-limited productivity in stratified waters. Similarly, the North Atlantic was also highly stratified with significantly reduced NADW production (Poli et al., 2010). High stratification appears to have led to lowered productivity in both the Atlantic and Pacific.

Sea level was low during this interval (Rohling et al., 2010), placing U1345 proximal to the Beringian coast (Fig. 2). With the Beringian shelf exposed, the continent was relatively cold and arid (Glushkova, 2001). In western Beringia, Lake El'gygytgyn was perennially covered with ice, summer air temperatures were warming from 4 to 12° C and annual precipitation was low (200-400 mm) (Vogel et al., 2013).

Numerous shell fragments, two sand layers and the highest percentages of clay-sized sediments in the record were deposited during MIS 12 (Fig.s 4 and 8) indicating input of terrigenous material, however, both C/N and $\delta^{13}C$ indicate that the organic matter during MIS 12 is of marine origin. Non-organic, terrigenous material could be transported to U1345 by large glacial meltwater rivers, icebergs, or sea ice. It is unlikely that meltwater rivers played a large role in sediment transport at this time because terrigenous organic matter and fresh water diatoms are absent and there are only moderate amounts of

Clim. Past Discuss., doi:10.5194/cp-2015-184, 2016
Manuscript under review for journal Clim. Past
Published: 19 January 2016

609 diatoms transported from shallow waters (Fig. 8). This may also reflect the reduced area
610 of submerged continental shelf. In addition, glacial ice was likely restricted to mountain-
611 valley glaciers, similar to the last glacial maximum (e.g. Glushkova, 2001). These small,
612 distant glaciers would not have produced large amounts of ice bergs though occasional
613 glacial ice rafted debris (IRD) may have come from the Koryak Mountains, Aleutians or
614 Beringia. Consistent with this, sediments typical of glacial IRD, such as dropstones, are
615 sparse. Terrigenous materials found in MIS12 sediments are most likely evidence of sea
616 ice rafting which tends to preferentially entrain clay and silt (Reimnitz et al., 1998) or of
617 minor downslope transport. In contrast, the North Atlantic is surrounded by ice sheets
618 readily calving ice bergs and MIS 12 is characterized as an intense glacial period with ice
619 rafted debris found as far south as Bermuda (Poli et al., 2000). Evidence for warming and
620 the reduction of IRD begins as early as 430 ka in the North Atlantic (Kandiano et al.,
621 2012) and the strength of the Gulf Stream increases in step with this glacial ice loss
622 (Chaisson et al., 2002).

623

624 **5.2 Early MIS 11: Termination V (425-423 ka)**

625 Termination V is the transition from MIS 12 to MIS 11. Worldwide, it is a rapid
626 deglaciation that is followed by a long (up to 30 kyrs) climate optimum (Milker et al.,
627 2013). At U1345, it can be broken into two stages, the first part from 425-423 ka, and the
628 second part from 423-410 ka, which is notably dominated by laminated sediments and is
629 discussed in the next section. The first part of Termination V corresponds with a local
630 maxima in insolation at 65°N (Schimmelmann et al., 1990) and increasing temperatures
631 in Antarctica (EPICA community members, 2004), the North Atlantic (Voelker et al.,
632 2010), and globally (Milker et al., 2013).

633 At U1345, the first part of Termination V is expressed as increasing absolute diatom
634 abundances and relative percent abundance of *Chaetoceros* RS while sea ice diatoms and
635 $\delta^{15}N$ values decrease (Fig. 7) indicating gradually increasing productivity coupled with
636 decreasing nutrient utilization and sea ice.

637 At the same time, episodic increases in productivity were occurring in places as distant as
638 Lake Baikal (Prokopenko et al., 2010) and the North Atlantic (Chaisson et al., 2002;

Clim. Past Discuss., doi:10.5194/cp-2015-184, 2016
Manuscript under review for journal Clim. Past
Published: 19 January 2016

639 Dickson et al., 2009; Poli et al., 2010) and NADW formation was intensifying (Poli et al.,
640 2010). Ventilation of NADW generally continues to increase from 424 to 410 ka to its
641 strongest and then weakens over the course of the interglacial (Thunell et al., 2002). In
642 addition, the flux of terrigenous dust was decreasing near Antarctica reflecting perhaps a
643 decrease in the strength of Southern Ocean winds (Wolff et al., 2006). Evidence for
644 higher productivity in the Bering Sea, possibly caused by intensified upwelling, suggests
645 teleconnections between NADW formation, the strength of the southern winds, upwelling
646 in the North Pacific, and northward flow through Bering Strait (e.g. DeBoer and Nof,
647 2004).

648

649 **5.2.1 Early MIS 11, part 2: Laminations (423-410 ka)**

650 The most prominent expression of Termination V is a 3.5 m thick laminated interval
651 deposited beginning at 423 ka (Fig. 7) when insolation was high at 65°N (Berger and
652 Loutre, 1991). Its presence indicates that the bottom water at 1,000 m in the Bering Sea
653 was dysoxic for more than 11 kyrs. These laminations are characterized as Type I
654 laminations with a notably high diatom content (Fig. 4). Several lines of evidence point
655 towards high productivity among multiple phytoplankton groups as opposed to simply a
656 change in preservation. There is a two orders of magnitude increase in diatom
657 abundances since MIS 12, a low-diversity diatom assemblage dominated by *Chaetoceros*
658 RS, an abrupt increase in percent organic carbon, high percent $CaCO_3$ and abundant
659 calcareous nannofossils dominated by small *Gephyrocapsa.* Furthermore, enriched $\delta^{15}N$
660 values indicate increased nitrogen utilization that likely fed this increased productivity
661 (Fig. 7).

662 Sea ice is reduced during this interval with almost no epontic diatoms present and
663 reduced amounts of other sea ice diatoms (Fig. 7). The $\delta^{13}C$ pattern of depleted values at
664 the start of the laminated interval and increasingly enriched values until about 409 ka is
665 very similar to the C_{org}/N story (Fig. 7) reflecting the highest contribution from C3 plant
666 organic matter at the onset of the laminated interval as the tundra-covered Bering Shelf is
667 flooded. However, the depletion in $\delta^{13}C$ during the Termination V Laminations occurs at

Clim. Past Discuss., doi:10.5194/cp-2015-184, 2016
Manuscript under review for journal Clim. Past
Published: 19 January 2016

668 the same time that *Chaetoceros* RS overtake the assemblage (Fig. 7), so a species effect
669 cannot be ruled out.

670 The diatom record, on the other hand has the lowest contribution of neritic diatoms
671 during the laminated interval and virtually no fresh water diatoms (Fig. 7), suggesting
672 that although terrigenous organic matter was an important input at the site, coastal, river,
673 or swamp/tundra diatoms were not major constituents of this terrigenous organic matter.

674 The sum of this evidence of high productivity, reduced sea ice, and terrigenous input is
675 similar to changes in productivity in this region during Termination I (Brunelle et al.,
676 2007; Caissie et al., 2010). At the start of Termination I, productivity initially increased
677 while nitrogen utilization decreased, then an abrupt increase in productivity and nitrogen
678 utilization was recorded (Brunelle et al., 2007; Brunelle et al., 2010). It is plausible that
679 increased nitrogen availability drove higher primary productivity as floods scoured fresh
680 organic matter from the submerging continental shelf (Bertrand et al., 2000). Rapid input
681 of bioavailable nitrogen as the shelf was inundated has been suggested to explain
682 increasing productivity during the last deglaciation in the Sea of Okhotsk (Shiga and
683 Koizumi, 2000) and during MIS 11 in the North Atlantic (Poli et al., 2010) and also may
684 have contributed to dysoxia by ramping up nutrient recycling, bacterial respiration, and
685 decomposition of organic matter in the Bering Sea.

686 The brief nitrogen utilization decrease just prior to the laminations (Fig. 7), suggests that
687 productivity was limited by some other factor, such as light or micronutrients, and could
688 not increase proportional to the increase in available nitrogen. Lam (2013) suggests that
689 during the last deglaciation, a breakdown in stratification limited productivity by creating
690 a very deep mixed layer that extended below the photic zone. This seems possible during
691 Termination V, since diatom indicators for stratified waters (dicothermal species) and
692 epontic diatoms decline coeval with the increase in productivity indicators (Fig. 7),
693 though seasonal sea ice remains and likely provides a mechanism for maintaining
694 stratification to some extent. As the interglacial began however, we would expect this
695 light limitation to be removed when stratification was re-established. However, if
696 dicothermal diatoms are indicators for stratification, then stratification is not re-
697 established until long after $\delta^{15}N$ values increase (Fig. 7), suggesting that if there is a limit

Clim. Past Discuss., doi:10.5194/cp-2015-184, 2016
Manuscript under review for journal Clim. Past
Published: 19 January 2016

on productivity during the early deglacial it is likely not light via a deep mixed layer (Obata et al., 1996). In contrast, a nearby core (HLY 0202 JPC3) displayed laminated sediments for only about 500 years during the last deglaciation (Cook et al., 2005), suggesting that the two Terminations were very different.

There is a "Younger Dryas-like" temperature reversal seen midway through Termination V in the North Atlantic (Voelker et al., 2010), Antarctica (EPICA community members, 2004) and at Lake El'gygytgyn (Vogel et al., 2013), however there is no evidence for such an event in the Bering Sea.

5.3 Peak MIS 11 (423-394 ka)

Globally, peak interglacial conditions (often referred to as MIS 11.3 or 11c) are centered around 410 ka, though the exact interval of the temperature optimum varies and lasted anywhere from 10 to 30 kyrs (Kandiano et al., 2012; Kariya et al., 2010; Milker et al., 2013). At U1345, peak interglacial conditions begin during the Termination V Laminations and continue until 394 ka.

Both decreasing C_{org}/N and increasing $\delta^{13}C$ indicate that input of terrigenous organic matter decreases from the onset of the Termination V Laminations until mid MIS 11 (400 ka) at which time the organic matter remains solidly marine sourced for the remainder of the record (Fig. 7). Sea level is high and the Pacific water indicator, *N. seminae*, is found at the site beginning at 424 ka.

Throughout MIS 11, *Chaetoceros* RS, a species indicative of high productivity, is generally higher when insolation is higher and lower when isolation is lower (390-404 ka; Fig. 7). However, although their fluctuations are small, warm water species show the opposite trend, with higher proportions of warm water diatoms when insolation is low (Fig. 7). If higher proportions of warm water diatoms indicate warmer water, then this suggests that productivity is highest in colder waters but when insolation is high, and lowest in warmer waters when insolation is low.

During MIS 11c, global ice volume was the lowest that it has been for the past 500 kyrs (Lisiecki and Raymo, 2005), and generally continental temperatures were warmer than

Clim. Past Discuss., doi:10.5194/cp-2015-184, 2016
Manuscript under review for journal Clim. Past
Published: 19 January 2016

today (D'Anjou et al., 2013; de Vernal and Hillaire-Marcel, 2008; Lozhkin and Anderson, 2013; Lyle et al., 2001; Melles et al., 2012; Pol, 2011; Prokopenko et al., 2010; Raynaud et al., 2005; Tarasov et al., 2011; Tzedakis, 2010; Vogel et al., 2013) with a northward expansion of boreal forests in Beringia (Kleinen et al., 2014). However, it was not warm uniformly world-wide. At U1345, the relative percent warm water species suggest that SSTs during MIS 11c were only slightly warmer than during MIS 12. Indeed, MIS 11 is not the warmest interglacial in most marine records (Candy et al., 2014). This is especially evident in the Nordic Seas where MIS 11 SSTs were lower than Holocene values, although no IRD was deposited between 408 and 398 ka (Bauch et al., 2000).

However, MIS 11c was very humid in many places. In the Bering Sea, modeling studies estimate up to 50 mm more precipitation than today at 410 ka (Kleinen et al., 2014). The most humid, least continental period recorded in the sediments at Lake Baikal occurs from 420-405 ka (Prokopenko et al., 2010), and extremely high precipitation are recorded at Lake El'gygytgyn on the nearby Chukotka Peninsula from 420-400 ka (Melles et al., 2012). Conditions in Africa during MIS 11c were similar to the Holocene African humid period. In addition, pollen records from Western Europe also reflect humid environments (Candy et al., 2014). A warmer, moister climate in Western Europe and Africa is indicative of increased Atlantic Meridional Overturning Circulation (AMOC) (Bauch, 2013). AMOC appears to be stable over MIS 11 (Milker et al., 2013) as evidenced by high carbonate in the North Atlantic (Chaisson et al., 2002; Poli et al., 2010). Interestingly, small carbonate peaks in the Bering Sea are contemporaneous with those on the Bermuda Rise, suggesting teleconnections between the two regions (Fig. 7). These conditions are similar to a modern day negative North Atlantic Oscillation (NAO) which is linked to wet conditions in N. Africa, weaker westerlies, more zonal storm tracks, a dry Northern Europe, colder Nordic Seas and increased sea ice in the North Atlantic (Kandiano et al., 2012).

5.3.1 Bering Strait Current Reversal (406-402 ka)

Between 405 and 394 ka, there is an unusual diatom assemblage and grain size distribution at Site U1345. There are several possible explanations for deposition of

Clim. Past Discuss., doi:10.5194/cp-2015-184, 2016
Manuscript under review for journal Clim. Past
Published: 19 January 2016

shallow water and fresh water species along with large changes in sediment grain size. We will consider two possibilities in detail: Bering Strait current reversal and glacial surge in Beringia.

On St. Lawrence Island in the Northern Bering Sea (Fig. 1), evidence for Arctic mollusks entering the Gulf of Anadyr suggests that flow through Bering Strait was reversed at some point during the Middle Pleistocene (Hopkins, 1972). Unfortunately, this event is poorly dated. If Bering Strait flow were reversed due to a meltwater event (DeBoer and Nof, 2004), we would expect a temporary reduction in NADW formation and an increase in southerly winds from Antarctica (DeBoer and Nof, 2004). In the Bering Sea, we would expect to see an increase in common Arctic or Bering Strait diatom species and a decrease in North Pacific indicators. In addition, the clay minerals in the Arctic Ocean are overwhelmingly dominated by illite (Ortiz et al., 2012), which is a clay mineral that tends to adsorb large amounts of ammonium (Schubert and Calvert, 2001). So, if net flow were to the south, one might also expect to find decreased C_{org}/N and $\delta^{15}N$ values resulting from increased illite deposition.

A warm Arctic Ocean during MIS 11 suggests increased Pacific water input through Bering Strait (Cronin et al., 2013). Proxy evidence for NADW ventilation (decreases in $CaCO_3$ % and $\delta^{13}C$) indicates that between 412 and 392 ka, NADW formation decreased for short periods (< 1 ka) (Poli et al., 2010). In contrast, AABW formation appears to have drastically slowed around 404 ka, suggesting that winds derived from Antarctica decreased as opposed to increased (Hall et al., 2001).

At U1345, C_{org}/N values began decreasing linearly starting at 409 ka, productivity sharply decreases at 406 ka, $\delta^{15}N$ values are the most depleted at 405 ka, just 1 kyr before a conspicuous peak in *P. sulcata,* a common diatom in the Bering Strait. Finally, diversity is highest around 400 ka, due to the multiple contributions of Arctic species (fresh water, shelf, coastal, sea ice) and common pelagic diatoms, while the North Pacific indicator, *N. seminae* maintains low relative abundances throughout this interval. The sum of this evidence does point toward species migration from the Arctic Ocean southward. However, these changes occur in series over 4 kyrs or more and there is no synchronicity between NADW formation and Antarctic winds. Therefore, there is no consensus in the

Clim. Past Discuss., doi:10.5194/cp-2015-184, 2016
Manuscript under review for journal Clim. Past
Published: 19 January 2016

787 evidence to support or reject the hypothesis of reversed flow through Bering Strait during
788 MIS 11.

789

790 **5.3.2 Glacial Inception in Beringia (405-394 ka)**

791 Regardless of whether flow through Bering Strait reversed during peak MIS 11, the
792 interval between 405 and 394 ka contains an unusual diatom assemblage and grain size
793 distribution. Diatom assemblages are similar to that found in sediments from the
794 Anvillian Transgression 800 km northeast of U1345 near Kotzebue (Fig. 1) (Pushkar et
795 al., 1999). In the Bering Sea, a large peak in neritic species occurs at 404 ka followed by
796 the highest relative percentages of fresh water species at the site and a slight increase in
797 sea ice diatoms from 400 to 394 ka (Fig. 7).

798 Despite the deposition of shallow and fresh water species, the proportion of marine to
799 terrestrial carbon was the highest in the entire interval. However, primary productivity
800 was quite low during this interval with high nitrogen utilization reflected in the $\delta^{15}N$
801 values. Two large depletions in $\delta^{15}N$ bracket this interval and occur as *Chaetoceros* RS
802 decrease in relative percent abundance, but only the older depletion is also associated
803 with a decrease in the number of diatom valves per gram of sediment (Fig. 8). The older
804 depletion may reflect an environment that is limited by micronutrients such as iron as sea
805 level approaches its maximum.

806 Detailed grain size analysis shows a trend of increasing clay sized grains as well as a
807 broad increase in sand sized grains and in particular grains greater than 250 μm (Fig. 8).
808 All samples are poorly to very poorly sorted (See Supplemental Material). In addition,
809 shipboard data shows an increase in the presence of large, isolated clasts > 1 cm in
810 diameter, a cluster of sand layers (Fig. 8), and a thick interval of silty sand (Takahashi et
811 al., 2011) around 411 ka (Fig. 4).

812 The sum of this evidence leads us to propose that the interval highlighted in grey on
813 Figure 8, reflects a glacial advance that may be the onset of the Nome River Glaciation at
814 ~404 ka. This advance is short-lived in the Bering Sea and is followed by a period when
815 intensified winds blew fresh water diatoms more than 1000 km off shore to Site U1345.

Clim. Past Discuss., doi:10.5194/cp-2015-184, 2016
Manuscript under review for journal Clim. Past
Published: 19 January 2016

Glacial ice is effective at carrying terrigenous and near shore particles far from land. Previous work has suggested that sediments deposited by icebergs should be poorly sorted and skew towards coarser sediments (Nürnberg et al., 1994). Sediments greater than 150 μm are likely glacially ice rafted (St. John, 2008), however it is not possible to distinguish sediments deposited by glacial versus sea ice on grain size alone (St. John, 2008). Both types of ice commonly carry sand-sized or larger sediments (Nürnberg et al., 1994). Sea ice diatoms should not be found in glacial ice, instead, we would expect glacial ice to be either barren, or to carry fresh water diatoms from ice-scoured lake and pond sediments.

The Nome River Glaciation is the most extensive glaciation in central Beringia and is dated to Middle Pleistocene. Although it has not been precisely dated, it is likely correlative with MIS 11 (Kaufman et al., 1991; Miller et al., 2009). Nome River glaciomarine sediments are found in places such as St. Lawrence Island (Gualtieri and Brigham-Grette, 2001; Hopkins, 1972), the Pribilof Islands (Hopkins, 1966), the Alaska Arctic coastal plain (Kaufman and Brigham-Grette, 1993), Kotzebue (Huston et al., 1990), Nome (Kaufman, 1992), and Bristol Bay (Kaufman et al., 2001) (Fig. 1). Mollusks and pollen in these sediments reflect a tundra environment with temperatures similar to today (Hopkins, 1972; Kaufman and Brigham-Grette, 1993) or warmer than today (Pushkar et al., 1999) with significantly reduced or absent sea ice (Kaufman and Brigham-Grette, 1993; Pushkar et al., 1999). These sites all contain evidence that glaciers in Beringia advanced, in some cases more than 200 km, and reached tidewater while eustatic sea level was high (Huston et al., 1990).

Although global sea level was near its maximum, and much of the world was experiencing peak MIS 11 conditions (Candy et al., 2014), there is evidence that the high latitudes were already cooling. At 410 ka, insolation at 65° N began to decline (Berger and Loutre, 1991), cooling began at 407 ka in Antarctica, expressed both isotopically and as an expansion of sea ice (Pol, 2011). Millennial scale cooling events are recorded at Lake Baikal (Prokopenko et al., 2010). By 405 ka, there is some evidence globally for ice sheet growth (Milker et al., 2013) as Lake Baikal begins to shift towards a dryer, more continental climate (Prokopenko et al., 2010) and productivity declines at Lake El'gygytgyn (Melles et al., 2012). Around 400 ka, SSTs decrease temporarily by 2° C in

Clim. Past Discuss., doi:10.5194/cp-2015-184, 2016
Manuscript under review for journal Clim. Past
Published: 19 January 2016

847 the Arctic Ocean (Medeleev Ridge) (Cronin et al., 2013) and permanently at Lake
848 El'gygytgyn (D'Anjou et al., 2013). Precipitation also decreases at Lake El'gygytgyn
849 (Melles et al., 2012). Modelling results show that by 400 ka, the Bering Sea is expected
850 to have temperatures cooler than today with increased sea ice (Kleinen et al., 2014).

851 We suggest that Beringian glaciation during MIS 11 was initiated ~404 ka by decreasing
852 insolation when eccentricity was high and perihelion coincided with the equinox
853 (Schimmelmann et al., 1990). Solar forcing coupled with a proximal moisture source, the
854 flooded Beringian shelf, to drive snow buildup (Huston et al., 1990; Pushkar et al., 1999)
855 and glacial advance. Precipitation at Lake El'gygytgyn, just west of the Bering Strait, was
856 two to three times higher than today (Melles et al., 2012). A similar "snow gun"
857 hypothesis has been invoked for other high latitude glaciations (Miller and De Vernal,
858 1992); however, Beringia is uniquely situated. Once sea level began to drop, Beringia
859 became more continental and arid (Prokopenko et al., 2010) and the moisture source for
860 these glaciers was quickly cut off.

861 In central Beringia, glaciers from coastal mountains on chukotka advanced to St.
862 Lawrence Island and glaciers from the western Brooks Range advanced into Kotzebue
863 Sound as global eustatic sea level dropped coincident with decreased insolation during
864 Northern Hemisphere summers (Berger and Loutre, 1991), Lake El'gygytgyn returned to
865 glacial conditions by 398 ka, and globally MIS 11.3 ended (Milker et al., 2013; Poli et al.,
866 2010; Voelker et al., 2010).

867

868 ### 5.3.3 Alternative Explanations

869 There are several other explanations for how these sediments could have been carried
870 more than 300 km from the coast out over the shelf-slope break and deposited in 1000 m
871 of water: turbidites or strong density currents on the shelf, sediment reworking and
872 winnowing, sea ice transport, and eolian deposition

873 The location of Site U1345 on a high interfluve minimizes the likelihood that sediments
874 will have been transported and deposited here by turbidites or other down-slope currents.
875 Sancetta and Robinson (1983) argue that benthic pennate species were transported out of

Clim. Past Discuss., doi:10.5194/cp-2015-184, 2016
Manuscript under review for journal Clim. Past
Published: 19 January 2016

shallow water by rivers and turbidity currents during glacial periods. They do not consider ice as a transport mechanism (Sancetta and Robinson, 1983). If turbidites were present, we would expect fining up sequences in the detailed grain size analysis, slumping or distorted sedimentation in the core and clear erosive surfaces. But there is no evidence of turbidite deposition (Takahashi et al., 2011). If winnowing were a dominant transport mechanism, the sediments should be well sorted. Instead, the presence of multiple terrigenous grain sizes indicates that the sediments are relatively poorly sorted and the Folk and Ward method (Blott and Pye, 2001) classifies all samples as either poorly sorted or very poorly sorted (See supplemental material).

Sea ice could bring neritic (though probably not freshwater) diatoms out to deeper waters as it preferentially entrains silt and clay size particles (Reimnitz et al., 1998). However, if there was an increase in sea ice, we would expect to see a significant increase in sea ice diatoms during this interval. Instead we see only a small increase in sea ice related species, primarily epontic species. Additionally, during this time, the marginal ice zone assemblage is dominated by *T. antarctica* RS which is a taxon primarily found in coastal, low salinity areas (Barron et al., 2009; Shiga and Koizumi, 2000), so its presence may be further support for increased shelf to basin transport.

Eolian deposition of diatoms is a common event in Antarctica where strong katabatic winds transport mainly small (up to 50 µm in diameter), non-marine diatoms (McKay et al., 2008). The freshwater diatoms that are abundant between 409 and 405 ka are dominated by species that tend to be quite small. *Lindavia* cf. *ocellata* ranges from 8-20 µm and *Lindavia radiosa* from 7-35 µm. Wind-driven deposition of these species is the most probably explanation for their transport more than 800 km from shore, therefore, this interval may represent a period of time when northerly winds intensified over Beringia.

5.4 Late MIS 11 (younger than 394 ka)

After 394 ka, upwelling indicators are the lowest in the record and linearly increase to the top of the record. This is in contrast to a slight increase in diatom abundance, which increases at 393 ka and then remains relatively stable to the top of the record. Sea ice

Clim. Past Discuss., doi:10.5194/cp-2015-184, 2016
Manuscript under review for journal Clim. Past
Published: 19 January 2016

indicators also remain relatively high from 392 to the top of the record and dicothermal species reflect moderately stratified waters. Warm water species decrease from 390 ka to the top of the record (Fig. 7). The sum of this evidence indicates that at the end of MIS 11, summers were warm and sea ice occurred seasonally, perhaps lasting a bit longer than at other times in the record. Modelling results indicate that at 394 ka, temperatures were below modern by 0° to 2° C, and precipitation in Beringia was relatively low, like today (Kleinen et al., 2014). These patterns reflect general cooling worldwide (de Abreu et al., 2005; Prokopenko et al., 2010; Raynaud et al., 2005). IRD is again deposited in the North Atlantic beginning around 390 ka.

Eustatic sea level decreased beginning about 402 ka (Rohling et al., 2010), but sea level was high enough though to allow *N. seminae* to reach the shelf slope break until about 380 ka (Fig. 7). As sea level dropped, significant parts of the Beringian continental shelf were exposed, cutting off the moisture supply for the Nome River Glaciation (Pushkar et al., 1999). Subaerial and glaciofluvial deposits above the Nome River tills and correlative glaciations indicate that Beringian ice retreated, while climate remained cold or grew colder. Ice wedges and evidence of permafrost are common (Huston et al., 1990; Pushkar et al., 1999) above Nome River glaciation deposits.

Laminations are again prominent in the sediment record and deposited intermittently between 394 and 392 ka and again after 375 ka (Fig. 4) as the climate transitioned into MIS 10. These laminations are quite different from the Termination V Laminations due to their shorter duration and lack of obvious shift in terrigenous vs. marine carbon source. In addition, these Type II laminations have increased diatom abundances and $CaCO_3$, but not necessarily increased upwelling indicators reflecting increased primary production that is perhaps not linked to nutrient upwelling along the shelf-slope break.

Most of these laminations show an increase in sea ice diatoms and a decrease in productivity indicators. These roughly correspond with millennial scale stadial events that occurred during MIS 11a in the North Atlantic (Fig. 7) (Voelker et al., 2010). Late MIS 11 is characterized as a series of warm and cold cycles (Candy et al., 2014; Voelker et al., 2010), though there is not agreement on the timing of these cycles.

Clim. Past Discuss., doi:10.5194/cp-2015-184, 2016
Manuscript under review for journal Clim. Past
Published: 19 January 2016

It is tantalizing to note that the laminations occur at a time when global sea level was fluctuating around -50 mapsl (Rohling et al., 2010) (see grey line at -50 m on Fig. 7). Increased productivity and repeating laminated sediments could be related to shelf to basin nutrient dynamics as rising sea levels carry fresh organic matter from the shelf out over the southern Bering Sea (e.g. Bertrand et al., 2000). In addition to the correspondence between laminations and North Atlantic stadials, carbonate peaks in the Bering Sea also occur coeval with carbonate peaks at Blake Ridge (Chaisson et al., 2002) suggesting teleconnections between productivity in the Bering Sea and the North Atlantic at this time. This suggests that sea level fluctuation driven by the closure of Bering Strait may also be occurring at the end of MIS 11 as well as during the last glacial maximum (Hu et al., 2010), though this hypothesis requires further testing and rethinking of dynamic topography in the Bering Strait region over time.

6 Conclusions

The interval between glacial MIS 12 and MIS 10 is marked by large changes in productivity but minor changes in sea ice extent at the shelf slope break in the Bering Sea. There is inconclusive evidence for a reversal of the Bering Strait current at 405 ka, but evidence for teleconnections between the Atlantic and the North Pacific is strong when eustatic sea level fluctuated near the Bering Strait sill depth at the end of MIS 11. Tidewater glaciers advanced in Beringia when eustatic sea level was high, insolation was declining in the Arctic, and other high latitude regions saw decreasing SSTs.

During MIS 12, productivity and nitrogen utilization was low. At Termination V, an 11 kyr long laminated interval began. This interval was highly productive for multiple phytoplankton groups and diatom productivity increased by two orders of magnitude while nitrogen utilization decreased. The surface waters were relatively warm and unstratified with reduced sea ice duration. This period is marked by the highest terrigenous organic matter input of the record possibly due to scouring of the continental shelf as sea level rose. Throughout much of MIS 11, productivity changed in concert with changes in insolation and water temperature. During warmer periods, high stratification

Clim. Past Discuss., doi:10.5194/cp-2015-184, 2016
Manuscript under review for journal Clim. Past
Published: 19 January 2016

964 appears to have led to lowered productivity in both the Atlantic and the North Pacific
965 Oceans.

966 During MIS 12, seasonal sea ice dominated the western Bering Sea with highly stratified
967 waters during the ice-melt season. Sea ice was at a minimum from 423 to 410 ka when
968 the Termination V Laminations were deposited. After this, although summers appear to
969 have been warm, seasonal sea ice lasted longer. And at the end of MIS 11, sea ice
970 increased and cooling continued in sync with declining sea level.

971 While decreased NADW formation and species transport from the Arctic Ocean
972 southward support a reversal of the Bering Strait current at 405 ka, there is no evidence
973 for transport of Arctic Ocean clay minerals or an increase in winds in Antarctica. In
974 addition, oceanographic changes indicative of a shift in Bering Strait through flow occur
975 in series over 4 kyrs or more and there is no synchronicity with Bering Sea changes,
976 NADW formation and Antarctic winds. Therefore, there is inconclusive evidence for a
977 reversal of the Bering Strait current during MIS 11.

978 When global sea level was at its maximum, insolation dropped slightly and coastal
979 Beringia began to cool in sync with other polar regions. Tidewater glaciers brought
980 neritic species far off shore and are attributed to humid conditions in Beringia that
981 allowed glacial growth. Evidence of glaciation is short lived in the western Bering Sea
982 and followed by an intensification of northerly winds that brought freshwater diatoms out
983 over the open ocean.

984 Laminations at end MIS 11 correspond with millennial scale stadials seen in the N
985 Atlantic. These deposits represent further possible evidence of teleconnections between
986 the Atlantic and the Pacific as eustatic sea level fluctuated near the Bering Strait sill
987 depth.

988 This study supports hypotheses that the region responds to insolation changes at 65° N
989 and that Bering Strait modulates climate in both the North Atlantic and Pacific regions.
990 Future work should focus on leads and lags between changes in the North Atlantic, North
991 Pacific and Antarctic regions to determine how upwelling, deep water formation, and
992 climate are related.

Clim. Past Discuss., doi:10.5194/cp-2015-184, 2016
Manuscript under review for journal Clim. Past
Published: 19 January 2016

Data used in this manuscript are archived at the National Center for Environmental Information (doi and web address pending).

Acknowledgements

The authors thank the captain and crew of the JOIDES Resolution and Exp. 323 co-chief scientists Christina Ravelo and Kozo Takahashi. This work was partially supported by National Science Foundation, Office of Polar Programs Arctic Natural Sciences Award #1023537 and a Post Expedition Award from the Consortium for Ocean Leadership.

Clim. Past Discuss., doi:10.5194/cp-2015-184, 2016
Manuscript under review for journal Clim. Past
Published: 19 January 2016

References

Aizawa, C., Tanimoto, M., and Jordan, R. W.: Living diatom assemblages from North Pacific and Bering Sea surface waters during summer 1999, Deep-Sea Research Part Ii-Topical Studies in Oceanography, 52, 2186-2205, 2005.

Alexander, V. and Chapman, T.: The role of epontic algal communities in Bering Sea ice. In: The Eastern Bering Sea Shelf: Oceanography and Resources, Hood, D. W. and Calder, J. A. (Eds.), University of Washington Press, Seattle, Washington, 1981.

Armand, L. K., Crosta, X., Romero, O., and Pichon, J. J.: The biogeography of major diatom taxa in Southern Ocean sediments: 1. Sea ice related species, Palaeogeography, Palaeoclimatology, Palaeoecology, 223, 93-126, 2005.

Barron, J. A., Bukry, D., Dean, W. E., Addison, J. A., and Finney, B.: Paleoceanography of the Gulf of Alaska during the past 15,000 years: results from diatoms, silicoflagellates, and geochemistry, Marine Micropaleontology, 72, 176-195, 2009.

Bassinot, F. C., Labeyrie, L. D., Vincent, E., Quidelleur, X., Shackleton, N. J., and Lancelot, Y.: (Table 4) Isotopic event stack. In supplement to: The astronomical theory of climate and the age of the Brunhes-Matuyama magnetic reversal, Earth and Planetary Science Letters, 126, 91-108, 1994.

Bauch, H. A.: Interglacial climates and the Atlantic meridional overturning circulation: is there an Arctic controversy?, Quaternary Science Reviews, 63, 1-22, 2013.

Bauch, H. A., Erlenkeuse, H., Helmke, J. P., and Struck, U.: A paleoclimatic evaluatioun of marine oxygen isotope stage 11 in thehigh-northern Atlantic (Nordic seas), Global and Planetary Change, 24, 27-39, 2000.

Berger, A., Crucifix, M., Hodell, D. A., Mangili, C., McManus, J. F., Otto-Bliesner, B., Pol, K., Raynaud, D., Skinner, L. C., Tzedakis, P. C., Wolff, E. W., Yin, Q. Z., Abe-Ouchi, A., Barbante, C., Brovkin, V., Cacho, I., Capron, E., Ferretti, P., Ganopolski, A.,

1026 Grimalt, J. O., Hönisch, B., Kawamura, K., Landais, A., Margari, V., Martrat, B.,
1027 Masson-Delmotte, V., Mokeddem, Z., Parrenin, F., Prokopenko, A. A., Rashid, H.,
1028 Schulz, M., and Vazquez Riveiros, N.: "Interglacials of the last 800,000 years", Rev
1029 Geophys, doi: 10.1002/2015RG000482, 2015. n/a-n/a, 2015.

1030 Berger, A. and Loutre, M. F.: Insolation Values for the Climate of the Last 10 Million
1031 Years, Quaternary Science Reviews, 10, 297-317, 1991.

1032 Bertrand, P., Pedersen, T. F., Martinez, P., Calvert, S., and Shimmield, G.: Sea level
1033 impact on nutrient cycling in coastal upwelling areas during deglaciation: evidence from
1034 nitrogen isotopes, Global Biogeochemical Cycles, 14, 341-355, 2000.

1035 Blasco, D., Estrada, M., and Jones, B.: Relationship between the phytoplankton
1036 distribution and composition and the hydrography in the Northwest African upwelling
1037 region near Cabo Carboeiro, Deep Sea Research, 27A, 799-821, 1980.

1038 Blott, S. J. and Pye, K.: GRADISTAT: A grain size distribution and statistics package for
1039 the analysis of unconsolidated sediments, Earth Surface Processes and Landforms, 26,
1040 1237-1248, 2001.

1041 Bowen, D. Q.: Sea level ~400 000 years ago (MIS 11): analogue for present and future
1042 sea-level?, Clim Past, 6, 19-29, 2010.

1043 Brigham-Grette, J., Hopkins, D. M., Ivanov, V. F., Basilyan, A. E., Benson, S. L., Heiser,
1044 P. A., and Pushkar, V. S.: Last interglacial (isotope stage 5) glacial and sea-level history
1045 of coastal Chukotka Peninsula and St. Lawrence Island, Western Beringia, Quaternary
1046 Science Reviews, 20, 419-436, 2001.

1047 Brunelle, B. G., Sigman, D. M., Cook, M. S., Keigwin, L., Haug, G. H., Plessen, B.,
1048 Schettler, G., and Jaccard, S. L.: Evidence from diatom-bound nitrogen isotopes for
1049 subarctic Pacific stratification during the last ice age and a link to North Pacific
1050 denitrification changes, Paleoceanography, 22, 2007.

Clim. Past Discuss., doi:10.5194/cp-2015-184, 2016
Manuscript under review for journal Clim. Past
Published: 19 January 2016

1051 Brunelle, B. G., Sigman, D. M., Jaccard, S. L., Keigwin, L. D., Plessen, B., Schettler, G.,
1052 Cook, M. S., and Haug, G. H.: Glacial/interglacial changes in nutrient supply and
1053 stratification in the western subarctic North Pacific since the penultimate glacial
1054 maximum, Quaternary Science Reviews, 29, 2579-2590, 2010.

1055 Caissie, B. E., Brigham-Grette, J., Lawrence, K. T., Herbert, T. D., and Cook, M. S.: Last
1056 Glacial Maximum to Holocene sea surface conditions at Umnak Plateau, Bering Sea, as
1057 inferred from diatom, alkenone, and stable isotope records, Paleoceanography, 25,
1058 10.1029/2008pa001671, 2010.

1059 Candy, I., Schreve, D. C., Sherriff, J., and Tye, G. J.: Marine Isotope Stage 11:
1060 Palaeoclimates, palaeoenvironments and its role as an analogue for the current
1061 interglacial, Earth-Science Reviews, 128, 18-51, 2014.

1062 Chaisson, W. P., Poli, M. S., and Thunell, R. C.: Gulf Stream and Western Boundary
1063 Undercurrent variations during MIS 10 -12 at Site 1056, Blake-Bahama Outer Ridge,
1064 Marine Geology, 189, 79-105, 2002.

1065 Cook, M. S., Keigwin, L. D., and Sancetta, C. A.: The deglacial history of surface and
1066 intermediate water of the Bering Sea, Deep Sea Research II, 52, 2163-2173, 2005.

1067 Cook, M. S., Ravelo, A. C., Mix, A., Nesbitt, I. M., and Miller, N. V.: Tracing Bering
1068 Sea circulation with benthic foraminiferal stable isotopes during the Pleistocene, Deep
1069 Sea Research Part II: Topical Studies in Oceanography, In Press. In Press.

1070 Cooper, L. W., Whitledge, T. E., Grebmeier, J. M., and Wieingartner, T.: The nutrient,
1071 salinity, and stable oxygen isotope composition of Bering and Chukchi Seas waters in
1072 and near the Bering Strait, Journal of Geophysical Research, 102, 12563-12573, 1997.

1073 Cronin, T. M., Polyak, L., Reed, D., Kandiano, E. S., Marzen, R. E., and Council, E. A.:
1074 A 600-ka Arctic sea-ice record from Mendeleev Ridge based on ostracodes, Quaternary
1075 Science Reviews, 79, 157-167, 2013.

Clim. Past Discuss., doi:10.5194/cp-2015-184, 2016
Manuscript under review for journal Clim. Past
Published: 19 January 2016

1076 D'Anjou, R. M., Wei, J. H., Casteneda, I. S., Brigham-Grette, J., Petsch, S. T., and
1077 Finkelstein, D. B.: High-latitude environmental change during MIS 9 and 11:
1078 biogeochemical evidence from Lake El'gygytgyn, Far East Russia, Clim Past, 9, 567-581,
1079 2013.

1080 de Abreu, C., Abrantes, F. F., Shackleton, N. J., Tzedakis, P. C., McManus, J. F., Oppo,
1081 D. W., and Hall, M. A.: Ocean climate variability in the eastern North Atlantic during
1082 interglacial marine isotope stage 11: A partial analogue to the Holocene?,
1083 Paleoceanography, 20, 10.1029/2004PA001091, 2005.

1084 de Vernal, A. and Hillaire-Marcel, C.: Natural variability of Greenland climate,
1085 vegetation, and ice volume during the past million years, Science, 320, 1622-1625, 2008.

1086 DeBoer, A. M. and Nof, D.: The Exhaust Valve of the North Atlantic, Journal of Climate,
1087 17, 417-422, 2004.

1088 Dickson, A. J., Beer, C. J., Dempsey, C., Maslin, M. A., Bendle, J. A., McClymont, E. L.,
1089 and Pancost, R. D.: Oceanic forcing of the Marine Isotope Stage 11 interglacial, Nature
1090 Geoscience, 2, 428-433, 2009.

1091 Droxler, A. W., Alley, R. B., Howard, W. R., Poore, R. Z., and Burckle, L. H.: Unique
1092 and exceptionally long interglacial Marine Isotope Stage 11: window into Earth's warm
1093 future climate. In: Earth's Climate and Orbital Eccentricity: The Marine Isotope Stage 11
1094 Question, Droxler, A. W., Poore, R. Z., and Burckle, L. H. (Eds.), American Geophysical
1095 Union, Washington, DC, 2003.

1096 EPICA community members: Eight glacial cycles from an Antarctic ice core, Nature,
1097 429, 623-628, 2004.

1098 Flores, J. A., Gersonde, R., and Sierro, F. J.: Pleistocene fluctuations in the Agulhas
1099 Current Retroflection based on the calcareous plankton record, Marine
1100 Micropaleontology, 37, 1-22, 1999.

Clim. Past Discuss., doi:10.5194/cp-2015-184, 2016
Manuscript under review for journal Clim. Past
Published: 19 January 2016

1101 Flores, J. A. and Sierro, F. J.: Revised technique for calculation of calcareous nannofossil
1102 accumulation rates, Micropaleontology, 43, 321-324, 1997.

1103 Fryxell, G. A. and Hasle, G. R.: *Thalassiosira eccentrica* (Ehreb.) Cleve, *T. symmetrica*
1104 sp. nov., and some related centric diatoms, Journal of Phycology, 8, 297-317, 1972.

1105 Glushkova, O. Y.: Geomorphological correlation of Late Pleistocene glacial complexes
1106 of Western and Eastern Beringia, Quaternary Science Reviews, 20, 405-417, 2001.

1107 Gualtieri, L. and Brigham-Grette, J.: The age and origin of the Little Diomede Island
1108 upland surface, Arctic, 54, 12-21, 2001.

1109 Håkansson, H.: A compilation and evaluation of species in the general *Stephanodiscus,*
1110 *Cyclostephanos,* and *Cyclotella* with a new genus in the family Stephanodiscaceae,
1111 Diatom Research, 17, 1-139, 2002.

1112 Hall, I. R., McCave, L. N., Shackleton, N. J., Weedon, G. P., and Harris, S. E.:
1113 Intensified deep Pacific inflow and ventilation in Pleistocene glacial times, Nature, 412,
1114 809-812, 2001.

1115 Hasle, G. R. and Heimdal, B. R.: Morphology and distribution of the marine centric
1116 diatom *Thalassiosira antarctica* Comber, Journal of the Royal Microscopical Society, 88,
1117 357-369, 1968.

1118 Hay, M. B., Dallimore, A., Thomson, R. E., Calvert, S. E., and Pienitz, R.: Siliceous
1119 microfossil record of late Holocene oceanography and climate along the west coast of
1120 Vancouver Island, British Columbia (Canada), Quaternary Research, 67, 33-49, 2007.

1121 Hopkins, D. M.: Cenozoic Hhistory of the Bering Land Bridge, Science, 129, 1519-1528,
1122 1959.

1123 Hopkins, D. M.: The paleogeography and climatic history of Beringia during late
1124 Cenozoic Time, Internord, 12, 121-150, 1972.

1125 Hopkins, D. M.: Pleistocene glaciation on St. George, Pribilof Islands, Science, 1966.
1126 343-345, 1966.

1127 Horner, R.: Sea Ice Biota, CRC Press, Inc, Boca Raton, FL, 1985.

1128 Hu, A. X., Meehl, G. A., Otto-Bliesner, B. L., Waelbroeck, C., Han, W. Q., Loutre, M.
1129 F., Lambeck, K., Mitrovica, J. X., and Rosenbloom, N.: Influence of Bering Strait flow
1130 and North Atlantic circulation on glacial sea-level changes, Nature Geoscience, 3, 118-
1131 121, 2010.

1132 Huston, M. M., Brigham-Grette, J., and Hopkins, D. M.: Paleogeographic significance of
1133 middle Pleistocene glaciomarine deposits on Baldwin Peninsula, northwestern Alaska,
1134 Annals of Glaciology, 14, 111-114, 1990.

1135 IPCC (Ed.): Climate Change 2013: The Physical Science Basis. Contribution of Working
1136 Group I to the Fifth Assessment Report of the Intergovernmental Panel on Climate
1137 Change, Cambridge University Press, Cambidge, U.K. and New York, NY, USA, 2013.

1138 Jouzel, J., Masson-Delmotte, V., Cattani, O., Dreyfus, G., Falourd, S., Hoffmann, G.,
1139 Minster, B., Nouet, J., Barnola, J. M., Chappellaz, J., Fischer, H., Gallet, J. C., Johnsen,
1140 S., Leuenberger, M., Loulergue, L., Luethi, D., Oerter, H., Parrenin, F., Raisbeck, G.,
1141 Raynaud, D., Schilt, A., Schwander, J., Selmo, E., Souchez, R., Spahni, R., Stauffer, B.,
1142 Steffensen, J. P., Stenni, B., Stocker, T. F., Tison, J. L., Werner, M., and Wolff, E. W.:
1143 Orbital and millennial Antarctic climate variability over the past 800,000 years, Science,
1144 317, 793-796, 2007.

1145 Kandiano, E. S., Bauch, H. A., Fahl, K., Helmke, J. P., Roehl, U., Perez-Folgado, M., and
1146 Cacho, I.: The meridional temperature gradient in the eastern North Atlantic during MIS

Clim. Past Discuss., doi:10.5194/cp-2015-184, 2016
Manuscript under review for journal Clim. Past
Published: 19 January 2016

1147 11 and its link to the ocean-atmosphere system, Palaeogeography Palaeoclimatology
1148 Palaeoecology, 333, 24-39, 2012.

1149 Kariya, C., Hyodo, M., Tanigawa, K., and Sato, H.: Sea-level variation during MIS 11
1150 constrained by stepwise Osaka Bay extensions and its relation with climatic evolution,
1151 Quaternary Science Reviews, 29, 1863-1879, 2010.

1152 Katsuki, K. and Takahashi, K.: Diatoms as paleoenvironmental proxies for seasonal
1153 productivity, sea-ice and surface circulation in the Bering Sea during the late Quaternary,
1154 Deep Sea Research II, 52, 2110-2130, 2005.

1155 Kaufman, D. S.: Aminostratigraphy of Pliocene-Pleistocene high-sea-level deposits,
1156 Nome coastal plain and adjacent nearshore area, Alaska, Geological Society of America
1157 Bulletin, 104, 40-52, 1992.

1158 Kaufman, D. S. and Brigham-Grette, J.: Aminostratigraphic correlations and
1159 paleotemperature implications, Pliocene-Pleistocene high sea-level deposits,
1160 Northwestern Alaska, Quaternary Science Reviews, 12, 21-33, 1993.

1161 Kaufman, D. S., Manley, W. F., Forman, S. L., and Layer, P. W.: Pre-Late-Wisconsin
1162 glacial history, coastal Ahklun Mountains, southwestern Alaska - new amino acid,
1163 thermoluminescence, and $^{40}Ar/^{39}Ar$ results, Quaternary Science Reviews, 20, 337-352,
1164 2001.

1165 Kaufman, D. S., Walter, R. C., Brigham-Grette, J., and Hopkins, D. M.: Middle
1166 Pleistocene age of the Nome River glaciation, northwestern Alaska, Quaternary
1167 Research, 36, 277-293, 1991.

1168 Kim, S., Takahashi, K., Khim, B.-K., Kanematsu, Y., Asahi, H., and Ravelo, A. C.:
1169 Biogenic opal production changes during the Mid-Pleistocene Transition in the Bering
1170 Sea (IODP Expedition 323 Site U1343), Quaternary Research, 81, 151-157, 2014.

1171 Kindler, P. and Hearty, P. J.: Elevated marine terraces from Eleuthera (Bahamas) and
1172 Bermuda: sedimentological, petrographic, and geochronological evidence for important
1173 deglaciation events during the middle Pleistocene, Global and Planetary Change, 24, 41-
1174 58, 2000.

1175 Kleinen, T., Hildebrandt, S., Prange, M., Rachmayani, R., Mueller, S., Bezrukova, E.,
1176 Brovkin, V., and Tarasov, P. E.: The climate and vegetation of Marine Isotope Stage 11-
1177 Model results and proxy-based reconstructions at global and regional scale, Quaternary
1178 International, 348, 247-265, 2014.

1179 Koizumi, I.: The Late Cenozoic diatoms of Sites 183-193, Leg 19 Deep Sea Drilling
1180 Project, Initial Reports of the Deep Sea Drilling Project, 19, 805-855, 1973.

1181 Kowalik, Z.: Bering Sea Tides. In: Dynamics of the Bering Sea, Loughlin, T. R. and
1182 Ohtani, K. (Eds.), Universtiy of Alaska Sea Grant, Fairbanks, AK, 1999.

1183 Lam, P. J., Robinson, L. F., Blusztajn, J., Li, C., Cook, M. S., McManus, J. F., and
1184 Keigwin, L. D.: Transient stratification as the cause of the North Pacific productivity
1185 spike during deglaciation, Nature Geoscience, 6, 622-626, 2013.

1186 Lisiecki, L. E. and Raymo, M. E.: A Pliocene-Pleistocene stack of 57 globally distributed
1187 benthic delta O-18 records, Paleoceanography, 20, 10.1029/2004PA001071, 2005.

1188 Lopes, C., Mix, A. C., and Abrantes, F.: Diatoms in northeast Pacific surface sediments
1189 as paleoceanographic proxies, Marine Micropaleontology, 60, 45-65, 2006.

1190 Loutre, M. F. and Berger, A.: Marine Isotope Stage 11 as an analogue for the present
1191 interglacial, Global and Planetary Change, 36, 209-217, 2003.

1192 Lozhkin, A. V. and Anderson, P.: Vegetation responses to interglacial warming in the
1193 Arctic: examples from Lake El'gygytgyn, Far East Russian Arctic, Clim Past, 9, 1211-
1194 1219, 2013.

Clim. Past Discuss., doi:10.5194/cp-2015-184, 2016
Manuscript under review for journal Clim. Past
Published: 19 January 2016

1195 Lundholm, N. and Hasle, G. R.: Are *Fragilariopsis cylindrus* and *Fragilariopsis nana*
1196 bipolar diatoms? Morphological and molecular analyses of two sympatric species, Nova
1197 Hedwigia, 133, 231-250, 2008.

1198 Lundholm, N. and Hasle, G. R.: *Fragilariopsis* (Bacillariophyceae) of the Northern
1199 Hemisphere--morphology, taxonomy, phylogeny and distribution, with a description of
1200 *F. pacifica* sp. nov., Phycologia, 49, 438-460, 2010.

1201 Lyle, M., Heusser, L., Herbert, T., Mix, A. C., and Barron, J.: Interglacial theme and
1202 variations: 500 k.y. of orbital forcing and associated responses from the terrestrial and
1203 marine biosphere, U.S. Pacific Northwest, Geology, 29, 1115-1118, 2001.

1204 Manley, W. F., Kaufman, D. S., and Briner, J. P.: Pleistocene glacial history of the
1205 southern Ahklun Mountains, southwestern Alaska: Soil-development, morphometric, and
1206 radiocarbon constraints, Quaternary Science Reviews, 20, 353-370, 2001.

1207 Maurer, B. A. and McGill, B. J.: Chapter 5: measurement of species diversity. In:
1208 Biological Diversity, Magurran, A. E. and McGill, B. J. (Eds.), Oxford University Press,
1209 New York, 2011.

1210 McKay, R. M., Barrett, P. J., Harper, M. A., and Hannah, M. J.: Atmospheric transport
1211 and concentration of diatoms in surficial and glacial sediments of the Allan Hills,
1212 Transantarctic Mountains, Palaeogeography, Palaeoclimatology, Palaeoecology, 260,
1213 168-183, 2008.

1214 McManus, J., Oppo, D. W., Cullen, J. L., and Healey, S.: Marine Isotope Stage 11 (MIS
1215 11): analog for Holocene and future climate. In: Earth's Climate and Orbital Eccentricity:
1216 The Marine Isotope Stage 11, Droxler, A. W., Poore, R. Z., and Burkle, L. H. (Eds.),
1217 Geophysical Monograph 137, American Geophysical Union, Washington, DC, 2003.

Clim. Past Discuss., doi:10.5194/cp-2015-184, 2016
Manuscript under review for journal Clim. Past
Published: 19 January 2016

1218 McQuoid, M. R. and Hobson, L. A.: A Holocene record of diatom and silicoflagellate
1219 microfossils in sediments of Saanich Inlet, ODP Leg 169S, Marine Geology, 174, 111-
1220 123, 2001.

1221 Medlin, L. K. and Hasle, G. R.: Some *Nitzschia* and related diatom species from fast ice
1222 samples in the Arctic and Antarctic, Polar Biology, 10, 451-479, 1990.

1223 Medlin, L. K. and Priddle, J.: Polar Marine Diatoms, British Antarctic Survey, Natural
1224 Environment Research Council, Cambridge, 1990.

1225 Melles, M., Brigham-Grette, J., Minyuk, P., Nowaczyk, N. R., Wennrich, V., DeConto,
1226 R. M., Anderson, P. M., Andreev, A. A., Coletti, A., Cook, T. L., Haltia-Hovi, E.,
1227 Kukkonen, M., Lozhkin, A. V., Rosen, P., Tarasov, P. E., Vogel, H., and Wagner, B.: 2.8
1228 Million years of Arctic climate change from Lake El'gygytgyn, NE Russia, Science,
1229 2012. 2012.

1230 Melnikov, I. A., Kolosova, E. G., Welch, H. E., and Zhitina, L. S.: Sea ice biological
1231 communities and nutrient dynamics in the Canada Basin of the Arctic Ocean, Deep-Sea
1232 Research Part I-Oceanographic Research Papers, 49, 1623-1649, 2002.

1233 Meyers, P. A.: Preservation of elemental and isotopic source identification of
1234 sedimentary organic matter, Chemical Geology, 114, 289-302, 1994.

1235 Milker, Y., Rachmayani, R., Weinkauf, M. F. G., Prange, M., Raitzsch, M., Schulz, M.,
1236 and Kucera, M.: Global and regional sea surface temperature trends during Marine
1237 Isotope Stage 11, Clim Past, 9, 2231-2252, 2013.

1238 Miller, G. H., Brigham-Grette, J., Anderson, L., Bauch, H. A., Douglas, M. A., Edwards,
1239 M. E., Elias, S. A., Finney, B. P., Funder, S., Herbert, T., Hinzman, L. D., Kaufman, D.
1240 K., MacDonald, G. M., Robock, A., Serreze, M. C., Smol, J. P., Spielhagen, R. F., Wolfe,
1241 A. P., and Wolff, E. W.: Temperature and precipitation history of the Arctic. In: Past

1242 Climate Variability and Change in the Arctic and at High Latitudes, Research, U. S. C. C.
1243 P. a. S. o. G. C. (Ed.), U.S. Geological Survey, Reston, VA, 2009.

1244 Miller, G. H. and De Vernal, A.: Will greenhouse warming lead to Northern Hemisphere
1245 ice-sheet growth?, Nature, 355, 244-246, 1992.

1246 Naish, T., Powell, R., Levy, R., Wilson, G., Scherer, R., Talarico, F., Krissek, L.,
1247 Niessen, F., Pompilio, M., Wilson, T., Carter, L., DeConto, R., Huybers, P., McKay, R.,
1248 Pollard, D., Ross, J., Winter, D., Barrett, P., Browne, G., Cody, R., Cowan, E., Crampton,
1249 J., Dunbar, G., Dunbar, N., Florindo, F., Gebhardt, C., Graham, I., Hannah, M., Hansaraj,
1250 D., Harwood, D., Helling, D., Henrys, S., Hinnov, L., Kuhn, G., Kyle, P., Laufer, A.,
1251 Maffioli, P., Magens, D., Mandernack, K., McIntosh, W., Millan, C., Morin, R.,
1252 Ohneiser, C., Paulsen, T., Persico, D., Raine, I., Reed, J., Riesselman, C., Sagnotti, L.,
1253 Schmitt, D., Sjunneskog, C., Strong, P., Taviani, M., Vogel, S., Wilch, T., and Williams,
1254 T.: Obliquity-paced Pliocene West Antarctic ice sheet oscillations, Nature, 458, 322-
1255 U384, 2009.

1256 Normack, W. R. and Carlson, P. R.: Giant submarine canyons: is size any clue to their
1257 importance in the rock record? In: Geological Society of America Special Paper, Chan,
1258 M. A. and Archer, A. W. (Eds.), Geological Society of America, Boulder, CO, 2003.

1259 Nürnberg, D., Wollenburg, I., Dethleff, D., Eicken, H., Kassens, H., Letzig, T., Reimnitz,
1260 E., and Thiede, J.: Sediments in Arctic Sea-Ice - Implications for Entrainment, Transport
1261 and Release, Marine Geology, 119, 185-214, 1994.

1262 Obata, A., Ishizaka, J., and Endoh, M.: Global verification of critical depth theory for
1263 phytoplankton bloom with climatological in situ temperature and satellite ocean color
1264 data, Journal of Geophysical Research, 101, 20657-20667, 1996.

1265 Onodera, J. and Takahashi, K.: Diatoms and siliceous flagellates (silicoflagellates,
1266 ebridians, and endoskeletal dinoflagellate *Actiniscus*) from the Subarctic Pacific,

1267 Memoirs of the Faculty of Sciences Kyushu University., Series D, Earth and Planetary
1268 Sciences, 31, 105-136, 2007.

1269 Ortiz, J. D., Nof, D., Polyak, L., St-Onge, G., Lisé-Pronovost, A., Naidu, S., Darby, D.,
1270 and Brachfeld, S.: The Late Quaternary Flow through the Bering Strait Has Been Forced
1271 by the Southern Ocean Winds, Journal of Physical Oceanography, 42, 2014-2029, 2012.

1272 Pike, J., Crosta, X., Maddison, E. J., Stickley, C. E., Denis, D., Barbara, L., and Renssen,
1273 H.: Observations on the relationship between the Antarctic coastal diatoms *Thalassiosira*
1274 *antarctica* Comber and *Porosira glacialis* (Grunow) Jorgensen and sea ice concentrations
1275 during the late Quaternary, Marine Micropaleontology, 73, 14-25, 2009.

1276 Pol, K.: Links between MIS 11 millennial to sub-millennial climate variability and long
1277 term trends as revealed by new high resolution EPICA Dome C deuterium data - A
1278 comparison with the Holocene, Clim Past, 7, 437-450, 2011.

1279 Poli, M. S., Meyers, P. A., and Thunell, R. C.: The western North Atlantic record of MIS
1280 13 to 10: Changes in primary productivity, organic carbon accumulation and benthic
1281 foraminiferal assemblages in sediments from the Blake Outer Ridge (ODP Site 1058),
1282 Palaeogeography, Palaeoclimatology, Palaeoecology, 295, 89-101, 2010.

1283 Poli, M. S., Thunell, R. C., and Rio, D.: Millenial-scale changes in North Atlantic Deep
1284 Water circulation during Marine Isotope Stages 11 and 12: linkage to Antarctic climate,
1285 Geology, 28, 807-810, 2000.

1286 Pollard, D. and DeConto, R. M.: Modelling West Antarctic ice sheet growth and collapse
1287 through the past five million years, Nature, 458, 329-U389, 2009.

1288 Prokopenko, A. A., Bezrukova, E. V., Khursevich, G. K., Solotchina, E. P., Kuzmin, M.
1289 I., and Tarasov, P. E.: Climate in continental interior Asia during the longest interglacial
1290 of the past 500 000 years: the new MIS 11 records from Lake Baikal, SE Siberia, Clim
1291 Past, 6, 31-48, 2010.

Clim. Past Discuss., doi:10.5194/cp-2015-184, 2016
Manuscript under review for journal Clim. Past
Published: 19 January 2016

1292 Pushkar, V. S., Roof, S. R., Cherepanova, M. V., Hopkins, D. M., and Brigham-Grette,
1293 J.: Paleogeographic and paleoclimatic significance of diatoms from Middle Pleistocene
1294 marine and glaciomarine deposits on Baldwin Peninsula, northwestern Alaska,
1295 Palaeogeography, Palaeoclimatology, Palaeoecology, 152, 67-85, 1999.

1296 Raymo, M. E. and Mitrovica, J. X.: Collapse of polar ice sheets during the stage 11
1297 interglacial, Nature, 483, 453-456, 2012.

1298 Raymo, M. E., Mitrovica, J. X., O'Leary, M. J., DeConto, R. M., and Hearty, P. J.:
1299 Departures from eustasy in Pliocene sea-level records, Nature Geoscience, 4, 328-332,
1300 2011.

1301 Raynaud, D., Barnola, J. M., Souchez, R., Lorrain, R., Petit, J. R., Duval, P., and
1302 Lipenkov, V. Y.: The record for Marine Isotopic Stage 11, Nature, 436, 39-40, 2005.

1303 Redfield, A. C., Ketchum, B. H., and Richards, F. A.: The inuence of organisms on the
1304 composition of sea water. In: The Sea, Hill, M. N. (Ed.), Wiley, New ork, 1963.

1305 Reimnitz, E., McCormick, M., Bischof, J., and Darby, D. A.: Comparing sea-ice
1306 sediment load with Beaufort Sea shelf deposits: is entrainment selective?, Journal of
1307 Sedimentary Research, 68, 777-787, 1998.

1308 Rohling, E. J., Braun, K., Grant, K., Kucera, M., Roberts, A. P., Siddall, M., and
1309 Trommer, G.: Comparison between Holocene and Marine Isotope Stage-11 sea-level
1310 histories, Earth and Planetary Science Letters, 291, 97-105, 2010.

1311 Rohling, E. J., Fenton, M., Jorissen, F. J., Bertrand, P., Ganssen, G., and Caulet, J. P.:
1312 Magnitudes of sea-level lowstands of the past 500,000 years, Nature, 394, 162-165, 1998.

1313 Ryu, E., Lee, S. J., Yang, D. Y., and Kim, J. Y.: Paleoenvironmental studies of the
1314 Korean peninsula inferred from diatom assemblages, Quaternary International, 176-177,
1315 36-45, 2008.

Clim. Past Discuss., doi:10.5194/cp-2015-184, 2016
Manuscript under review for journal Clim. Past
Published: 19 January 2016

1316 Saito, K. and Taniguchi, A.: Phytoplankton communities in the Bering Sea and adjacent
1317 seas II: spring and summer communities in seasonally ice-covered areas, Astarte, 11, 27-
1318 35, 1978.

1319 Sancetta, C. A.: Distribution of diatom species in surface sediments of the Bering and
1320 Okhotsk seas, Micropaleontology, 28, 221-257, 1982.

1321 Sancetta, C. A.: Oceanographic and ecologic significance of diatoms in surface sediments
1322 of the Bering and Okhotsk seas, Deep Sea Research, 28A, 789-817, 1981.

1323 Sancetta, C. A.: Oceanography of the North Pacific during the Last 18,000 Years:
1324 Evidence from Fossil Diatoms, Marine Micropaleontology, 4, 103-123, 1979.

1325 Sancetta, C. A.: Three species of *Coscinodiscus* Ehrenberg from North Pacific sediments
1326 examined in the light and scanning electron microscopes, Micropaleontology, 33, 230-
1327 241, 1987.

1328 Sancetta, C. A. and Robinson, S. W.: Diatom evidence on Wisconsin and Holocene
1329 events in the Bering Sea, Quaternary Research, 20, 232-245, 1983.

1330 Sancetta, C. A. and Silvestri, S. M.: Diatom stratigraphy of the Late Pleistocene
1331 (Brunhes) Subarctic Pacific, Marine Micropaleontology, 9, 263-274, 1984.

1332 Sancetta, C. A. and Silvestri, S. M.: Pliocene-Pleistocene evolution of the North Pacific
1333 ocean-atmosphere system, interpreted from fossil diatoms, Paleoceanography, 1, 163-
1334 180, 1986.

1335 Schandelmeier, L. and Alexander, V.: An analysis of the influence of ice on spring
1336 phytoplankton population structure in the southeast Bering Sea, Limnology and
1337 Oceanography, 26, 935-943, 1981.

Clim. Past Discuss., doi:10.5194/cp-2015-184, 2016
Manuscript under review for journal Clim. Past
Published: 19 January 2016

1338 Scherer, R. P.: A new method for the determination of absolute abundance of diatoms
1339 and other silt-sized sedimentary particles, Journal of Paleolimnology, 12, 171-179, 1994.

1340 Scherer, R. P., Aldahan, A., Tulaczyk, S., Possnert, G., Engelhardt, H., and Kamb, B.:
1341 Pleistocene collapse of the West Antarctic Ice Sheet, Science, 281, 82-85, 1998.

1342 Schimmelmann, A., Lange, C. B., and Berger, W. H.: Climatically Controlled Marker
1343 Layers in Santa-Barbara Basin Sediments and Fine-Scale Core-to-Core Correlation,
1344 Limnology and Oceanography, 35, 165-173, 1990.

1345 Schrader, H. J. and Gersonde, R.: Diatoms and silicoflagellates. In: Micropaleontological
1346 counting methods and techniques - an exercise on an eight metres section of the Lower
1347 Pliocene of Capo Rossello, Sicily, Zachariasse, W. J., Riedel, W. R., Sanfilippo, A.,
1348 Schmidt, R. R., Brolsma, M. J., Schrader, H. J., Gersonde, R., Drooger, M. M., and
1349 Broekman, J. A. (Eds.), Utrecht Micropaleontological Bulletin, Netherlands, 1978.

1350 Schubert, C. J. and Calvert, S. E.: Nitrogen and carbon isotopic composition of marine
1351 and terrestrial organic matter in Arctic Ocean sediments: implications for nutrient
1352 utiliazation and organic matter composition, Deep Sea Research I, 48, 789-810, 2001.

1353 Schumacher, J. D. and Stabeno, P. J.: Continental shelf of the Bering Sea. In: The sea,
1354 Robinson, A. R. and Brink, K. H. (Eds.), John Wiley and Sons, New York, 1998.

1355 Shiga, K. and Koizumi, I.: Latest Quaternary oceanographic changes in the Okhotsk Sea
1356 based on diatom records, Marine Micropaleontology, 38, 91-117, 2000.

1357 Smol, J. P.: The paleolimnologist's Rosetta Stone: calibrating indicators to environmental
1358 variables using surface-sediment training sets. In: Pollution of lakes and rivers: a
1359 paleoenvironmental perspective, Smol, J. P. (Ed.), Key issues in environmental change,
1360 Oxford University Press, New York, 2002.

Clim. Past Discuss., doi:10.5194/cp-2015-184, 2016
Manuscript under review for journal Clim. Past
Published: 19 January 2016

1361 Springer, A. M., McRoy, C. P., and Flint, M. V.: The Bering Sea green belt: shelf edge
1362 processes and ecosystem production, Fisheries Oceanography, 5, 205-223, 1996.

1363 St. John, K.: Cenozoic ice-rafting history of the central Arctic Ocean: Terrigenous sands
1364 on the Lomonosov Ridge, Paleoceanography, 23, 10.1029/2007pa001483, 2008.

1365 Stabeno, P. J., Schumacher, J. D., and Ohtani, K.: The physical oceanography of the
1366 Bering Sea. In: Dynamics of the Bering Sea: a summary of physical, chemical, and
1367 biological characteristics, and a synopsis of research on the Bering Sea, Loughlin, T. R.
1368 and Ohtani, K. (Eds.), University of Alaska Sea Grant, Fairbanks, AK, 1999.

1369 Syvertsen, E. E.: Resting Spore Formation in Clonal Cultures of *Thalassiosira antarctica*
1370 Comber, *T. nordenskioeldii* Cleve and *Detonula confervacea* (Cleve) Gran, Nova
1371 Hedwigia, 64, 41-63, 1979.

1372 Takahashi, K., Ravelo, A. C., Alvarez Zarikian, C. A., and Scientists, E.: Proceedings of
1373 the Integrated Ocean Drilling Program. Tokyo, 2011.

1374 Tarasov, P. E., Nakagawa, T., Demske, D., Österle, H., Igarashi, Y., Kitagawa, J.,
1375 Mokhova, L., Bazarova, V., Okuda, M., Gotanda, K., Miyoshi, N., Fujiki, T., Takemura,
1376 K., Yonenobu, H., and Fleck, A.: Progress in the reconstruction of Quaternary climate
1377 dynamics in the Northwest Pacific: A new modern analogue reference dataset and its
1378 application to the 430-kyr pollen record from Lake Biwa, Earth-Science Reviews, 108,
1379 64-79, 2011.

1380 Ternois, Y., Kawamura, K., Keigwin, L., Ohkouchi, N., and Nakatsuka, T.: A biomarker
1381 approach for assessing marine and terrigenous inputs to the sediments of Sea of Okhotsk
1382 for the last 27,000 years, Geochimica et Cosmochimica Acta, 65, 791-802, 2001.

1383 Thunell, R., Poli, M. S., and Rio, D.: Changes in deep and intermediate water properties
1384 in the western North Atlantic during Marine Isotope Stages 11-12: evidence from ODP
1385 Leg 172, Marine Geology, 189, 63-77, 2002.

Clim. Past Discuss., doi:10.5194/cp-2015-184, 2016
Manuscript under review for journal Clim. Past
Published: 19 January 2016

1386 Tomas, C. R.: Identifying marine diatoms and dinoflagellates, Academic Press, Inc.
1387 Harcourt Brace and Co., Boston, U.S.A., 1996.

1388 Tzedakis, P. C.: The MIS 11 – MIS 1 analogy, southern European vegetation,
1389 atmospheric methane and the "early anthropogenic hypothesis", Clim Past, 6, 131-144,
1390 2010.

1391 van Hengstum, P. J., Scott, D. B., and Javaux, E. J.: Foraminifera in elevated Bermudian
1392 caves provide further evidence for +21m eustatic sea level during Marine Isotope Stage
1393 11, Quaternary Science Reviews, 28, 1850-1860, 2009.

1394 Voelker, A. H. L., Rodrigues, T., Billups, K., Oppo, D., McManus, J., Stein, R., Hefter,
1395 J., and Grimalt, J. O.: Variations in mid-latitude North Atlantic surface water properties
1396 during the mid-Brunhes (MIS 9–14) and their implications for the thermohaline
1397 circulation, Clim Past, 6, 531-552, 2010.

1398 Vogel, H., Meyer-Jacob, C., Melles, M., Brigham-Grette, J., Andreev, A. A., Wennrich,
1399 V., Tarasov, P. E., and Rosen, P.: Detailed insight into Arctic climatic variability during
1400 MIS 11c at Lake El'gygytgyn, NE Russia, Clim Past, 9, 1467-1479, 2013.

1401 von Quillfeldt, C. H.: Identification of some easily confused common diatom species in
1402 Arctic spring blooms, Botanica Marina, 44, 375-389, 2001.

1403 von Quillfeldt, C. H., Ambrose, W. G. J., and Clough, L. M.: High number of diatom
1404 species in first-year ice from the Chukchi Sea, Polar Biology, 26, 806-818, 2003.

1405 Witkowski, A., Lange-Bertalot, H., and Metzeltin, D.: Diatom Flora of Marine Coasts I,
1406 A.R.G. Gantner Verlag K.G., Ruggell, Liechtenstein, 2000.

1407 Wolff, E. W., Fischer, H., Fundel, F., Ruth, U., Twarloh, B., Littot, G. C., Mulvaney, R.,
1408 Rothlisberger, R., de Angelis, M., Boutron, C. F., Hansson, M., Jonsell, U., Hutterli, M.
1409 A., Lambert, F., Kaufmann, P., Stauffer, B., Stocker, T. F., Steffensen, J. P., Bigler, M.,

Clim. Past Discuss., doi:10.5194/cp-2015-184, 2016
Manuscript under review for journal Clim. Past
Published: 19 January 2016

1410 Siggaard-Andersen, M. L., Udisti, R., Becagli, S., Castellano, E., Severi, M., Wagenbach,
1411 D., Barbante, C., Gabrielli, P., and Gaspari, V.: Southern Ocean sea-ice extent,
1412 productivity and iron flux over the past eight glacial cycles, Nature, 440, 491-496, 2006.

1413 Young, J. R., Geisen, M., Cros, L., Keleijne, A., Sprengel, C., Probert, I., and
1414 Østengaard, J.: A guide to extant coccolithophore taxonomy, Journal of Nannoplankton
1415 Research, Special Issue, 1, 1-125, 2003.

1416 Zong, Y.: Implications of *Paralia sulcata* abundance in Scottish isolation basins, Diatom
1417 Research, 12, 125-150, 1997.
1418

Clim. Past Discuss., doi:10.5194/cp-2015-184, 2016
Manuscript under review for journal Clim. Past
Published: 19 January 2016

Climate of the Past Discussions
Open Access
EGU

1419 Table 1: Bering Sea diatom species grouped by environmental niche. In cases where a species appears in more than one niche, the
1420 grouping used in this study is highlighted in bold.

Modern Seasonal Succession			
Epontic	**Marginal Ice Zone (MIZ)**	**Both Epontic and MIZ**	**Summer Bloom**
Navicula transitrans	***Bacterosira bathyomphala***	*Actinocyclus curvatulus*	***Coscinodiscus* spp.**
Nitzschia frigida	*Chaetoceros furcellatus*	***Fossula arctica***	***Leptocylindrus* sp.**
	Chaetoceros socialis	***Fragilariopsis cylindrus***	***Rhizosolenia* spp.**
	Leptocylindrus sp.	***Fragilariopsis oceanica***	
	Odontella aurita	***Navicula pelagica***	
	Paralia sulcata	**Naviculoid pennates**	
	Porosira glacialis	***Nitzschia* spp.**	
	Staurosirella* cf. *pinnata	***Pinnularia quadratarea***	
	Thalassionema nitzschioides	***Thalassiosira antarctica***	
	Thalassiosira angulata	***Thalassiosira gravida***	
	Thalassiosira baltica		
	Thalassiosira decipiens		
	Thalassiosira hyalina		
	Thalassiosira hyperborea		
	Thalassiosira nordenskioeldii		
	Thalassiosira pacifica		

1421

1422 Continued on next page

Clim. Past Discuss., doi:10.5194/cp-2015-184, 2016
Manuscript under review for journal Clim. Past
Published: 19 January 2016

Climate of the Past Discussions
Open Access
EGU

Table 1 continued

Water Mass Tracers				*Shelf to Basin Transport*	
Dicothermal	**High Productivity**	**Alaska Stream**	**Warmer Water**	**Neritic**	**Fresh Water**
Actinocyclus curvatulus	***Chaetoceros* spp.**	***Neodenticula seminae***	***Azpeitia tabularis***	***Actinoptychus senarius***	***Lindavia* cf. *ocellata***
Thalassiosira trifulta	***Odontella aurita***		***Stellarimia* stellaris**	***Amphora* sp.**	*Lindavia stylorum*
	Thalassionema nitzschioides		*Thalassionema nitzschioides*	***Lindavia stylorum***	*Staurosirella* cf *pinnata*
	Thalassiosira pacifica		***Thalassiosira eccentrica***	***Delphineis spp.***	***Lindavia radiosa***
	***Thalassiosira* spp. small**		***Thalassiosira oestrupii***	***Dentonula confervacea***	
	Thalassiothrix longissima		***Thalassiosira symmetrica***	***Diploneis smithii***	
				Naviculoid pennates	
				Odontella aurita	
				Paralia sulcata	
				Rhaphoneis amphiceros	
				Stephanopyxis turris	
				Thalassiosira angulata	
				Thalassiosira decipiens	
				Thalassiosira eccentrica	

Clim. Past Discuss., doi:10.5194/cp-2015-184, 2016
Manuscript under review for journal Clim. Past
Published: 19 January 2016

Climate of the Past Discussions
Open Access
EGU

1424 Table 2: Distribution of Laminated Intervals during MIS 11. Note that the depth and age
1425 of laminated intervals encompasses all holes drilled, but the average duration is
1426 calculated using each of the holes that it is present in.

Lamination	Type	Depth (mbsf)	Age (ka)	Average Duration (kyrs)	Found in Holes
MIS 11.5	II	112.02-111.47	367.2-366.0	0.50	C
MIS 11.4	II	113.14-112.94	369.7-369.3	0.34	CD
MIS 11.3	II	114.28-113.95	372.3-371.5	0.73	D
MIS 11.2	II	115.59-114.69	374.8-373.2	1.25	ACE
MIS 11.1	II	121.84-121.18	394.1-392.1	1.10	ED
Termination V	I	130.00-126.52	423.3-410.4	12.14	ACDE

1437

Clim. Past Discuss., doi:10.5194/cp-2015-184, 2016
Manuscript under review for journal Clim. Past
Published: 19 January 2016

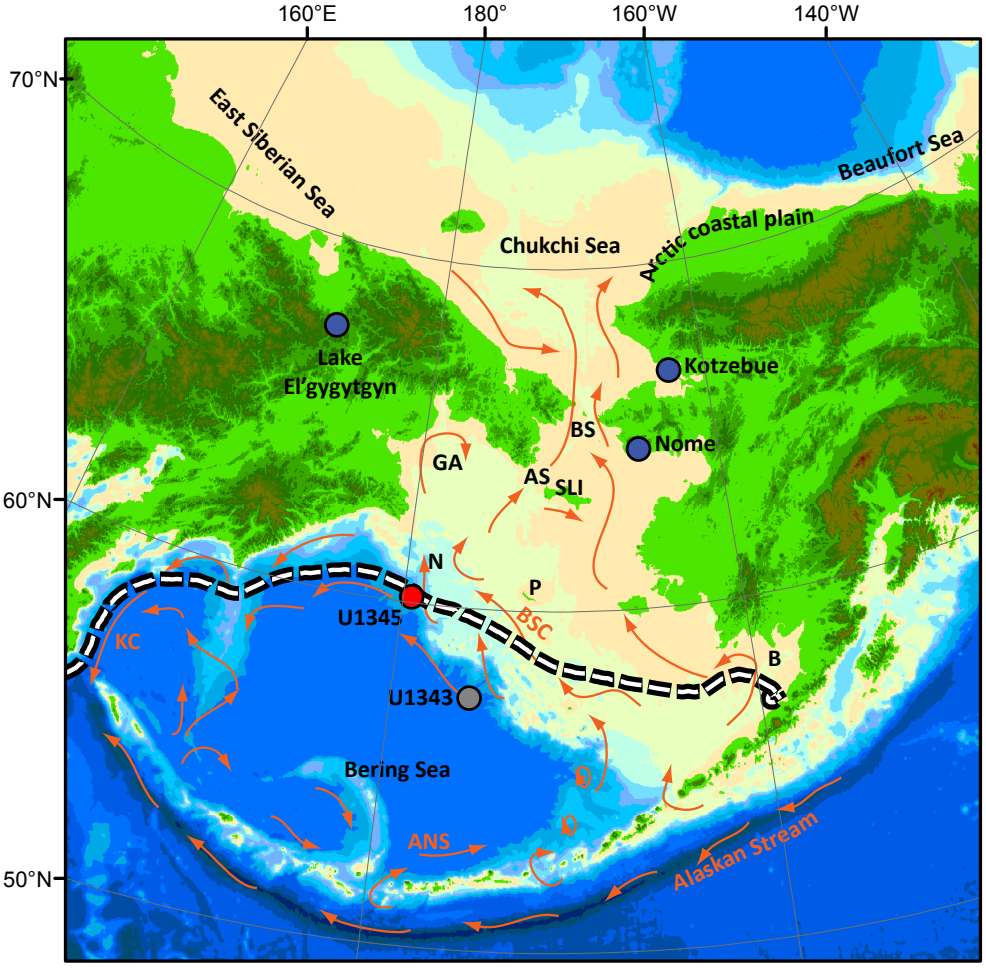

Figure 1. Map of Beringia. Locations of place names from the text are labeled: Aleutian North Slope Current (ANS), Anadyr Strait (AS), Bristol Bay (B), Bering Strait (BS), Bering Slope Current (BSC), Gulf of Anadyr (GA), Kamchatka Current (KC), Navarin Canyon (N), Pribilof Islands (P), St. Lawrence Island (SLI). The white and black dashed line is the modern, median maximum extent of sea ice (Cavalieri et al., 1996). Currents are in orange and are modified from Stabeno (Stabeno et al., 1999). Base map is modified from Manley (Manley, 2002).

Clim. Past Discuss., doi:10.5194/cp-2015-184, 2016
Manuscript under review for journal Clim. Past
Published: 19 January 2016

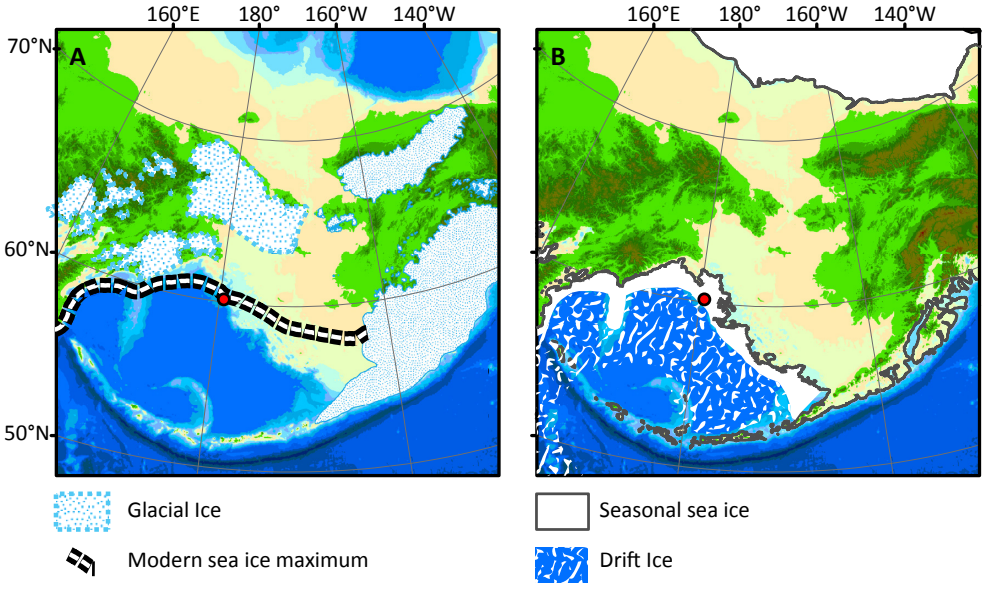

Figure 2. Maximum glacial and sea ice extents in Beringia. A. depicts the maximum glacial ice in Beringia as inferred from terminal and lateral moraines. This is not intended to show the maximum extent during a particular glaciation, but rather the maximum possible extent of glacial ice. These moraines are likely from several different major glaciations. The white and black dashed line is the modern, median maximum extent of sea ice (Cavalieri et al., 1996). B. depicts the approximate pattern of sea ice during glacial stages (Katsuki and Takahashi, 2005). The dark grey contour is -140 m, the approximate sea level during MIS 12 (Rohling et al., 2010). Base map is modified from Manley (Manley, 2002).

Clim. Past Discuss., doi:10.5194/cp-2015-184, 2016
Manuscript under review for journal Clim. Past
Published: 19 January 2016

Climate of the Past
Discussions
Open Access
EGU

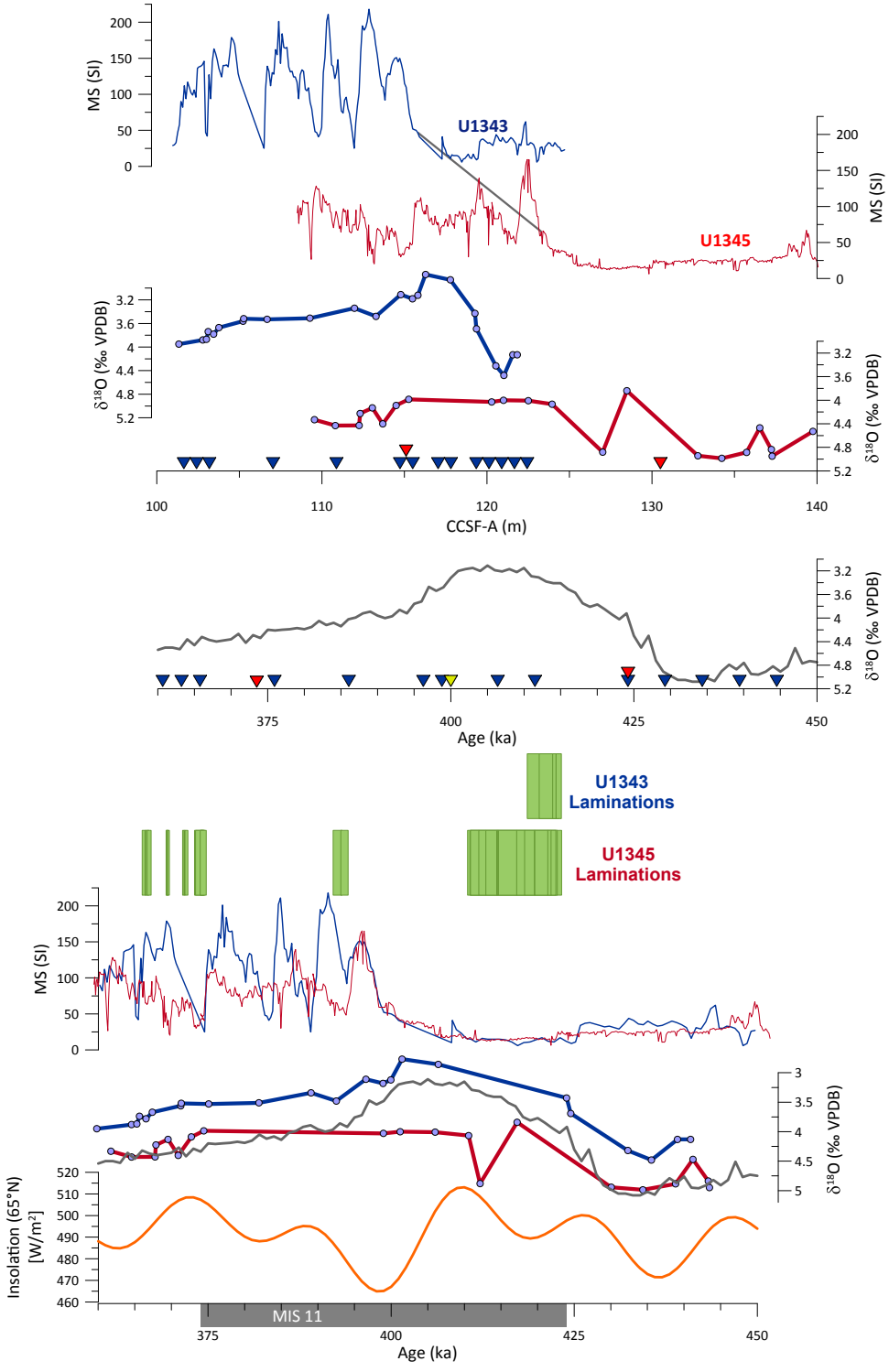

Clim. Past Discuss., doi:10.5194/cp-2015-184, 2016
Manuscript under review for journal Clim. Past
Published: 19 January 2016

Climate of the Past Discussions
Open Access
EGU

Figure 3. Age model. Blue plots depict data from Site U1343, red plots are from U1345. Magnetic susceptibility and benthic foraminiferal $\delta^{18}O$ are plotted by depth for each Site in the top half of the figure. The grey line joining the magnetic susceptibility plots indicates the tie point that was added in this study. Inverted triangles indicate locations of tie points between Bering Sea $\delta^{18}O$ (Cook et al., In Press; Kim et al., 2014) and the global marine stack (Lisiecki and Raymo, 2005), which is plotted in grey. Green bars indicate laminated intervals in U1343 and U1345 plotted by age. The bottom half of the figure depicts the same data (magnetic susceptibility and $\delta^{18}O$) plotted by age with the global marine stack (grey) and insolation at 65° N (orange for reference).

Clim. Past Discuss., doi:10.5194/cp-2015-184, 2016
Manuscript under review for journal Clim. Past
Published: 19 January 2016

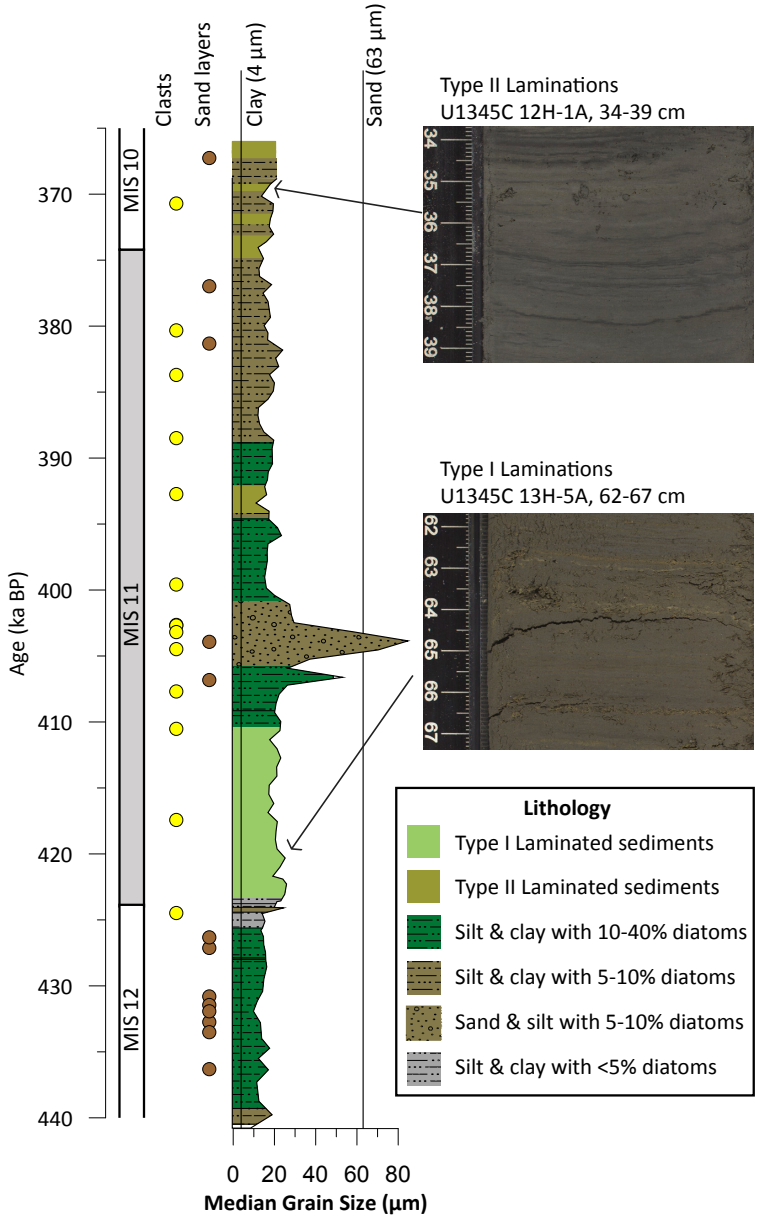

Figure 4. Lithostratigraphic column for U1345A. Marine Isotope Stage 11 is depicted as a grey bar. Ice rafted debris (yellow dots) and sand layers (maroon dots) are a compilation of these features in all four holes at U1345. The width of the lithologic column varies according to median grain size. Vertical lines indicate the cut off for clay and sand sized particles. Silt lies between the two lines. Colors depict varying amounts of diatoms relative to terrigenous grains in the sediment. Type I Laminations are depicted as pale green bars and Type II laminations are depicted as olive green bars. An example of each of the lamination types is shown in the images to the right.

Clim. Past Discuss., doi:10.5194/cp-2015-184, 2016
Manuscript under review for journal Clim. Past
Published: 19 January 2016

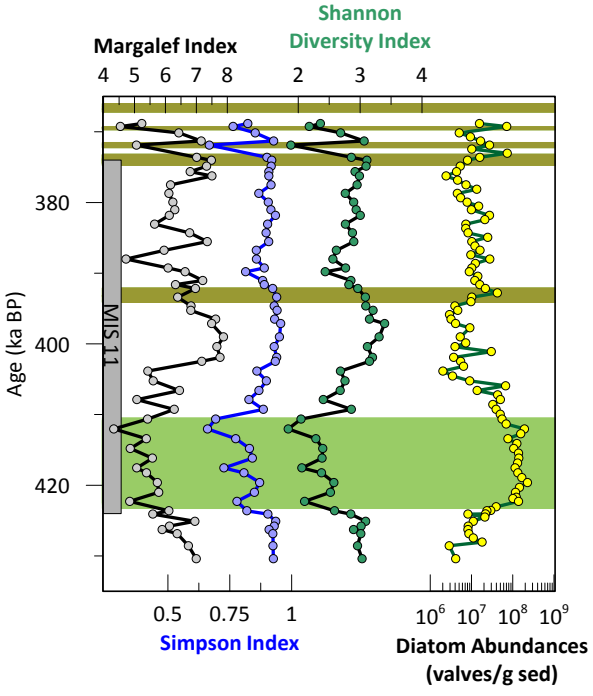

Figure 5. The Margalef, Simpson, and Shannon diversity indices plotted with diatom abundances. Type I Laminations are depicted as pale green bars and Type II laminations are depicted as olive green bars.

Clim. Past Discuss., doi:10.5194/cp-2015-184, 2016
Manuscript under review for journal Clim. Past
Published: 19 January 2016

Climate of the Past Discussions
Open Access
EGU

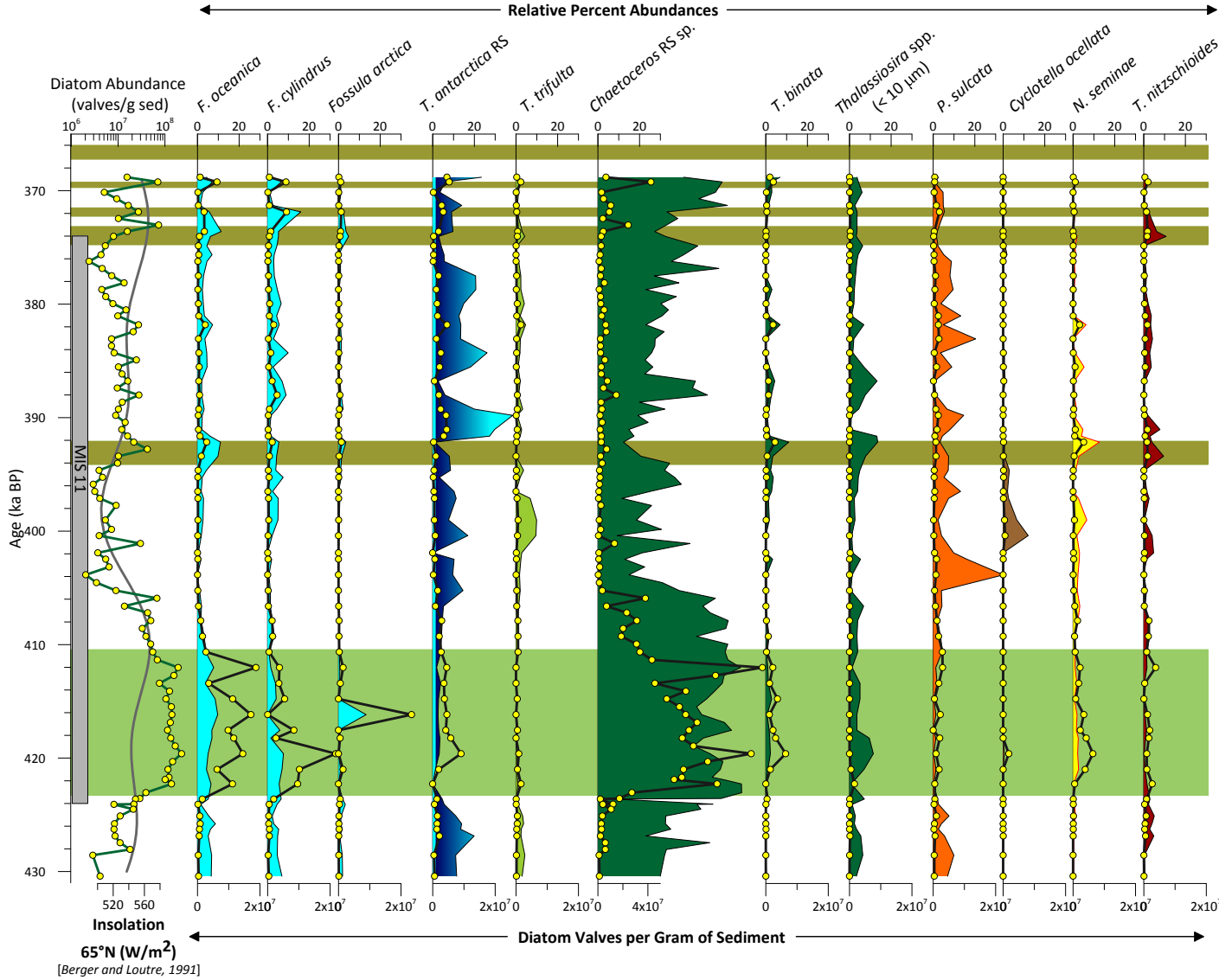

Clim. Past Discuss., doi:10.5194/cp-2015-184, 2016
Manuscript under review for journal Clim. Past
Published: 19 January 2016

Climate of the Past Discussions
Open Access
EGU

1449 Figure 6. Absolute and relative percent abundances of all diatoms that occur in
1450 abundances greater than 10% of any assemblage. Line plots depict absolute abundance
1451 and area plots depict relative percent abundance. Species are color coded according to the
1452 niche that they are grouped into: marginal ice zone (light blue), both ice types (dark blue
1453 to light blue), dicothermal (light green), high productivity (green), neritic (orange),
1454 freshwater (brown), North Pacific (yellow), and warm water (red). Insolation 65° N (light
1455 grey line) is also shown. Type I Laminations are depicted as pale green bars and Type II
1456 laminations are depicted as olive green bars.

Clim. Past Discuss., doi:10.5194/cp-2015-184, 2016
Manuscript under review for journal Clim. Past
Published: 19 January 2016

Climate of the Past Discussions
Open Access
EGU

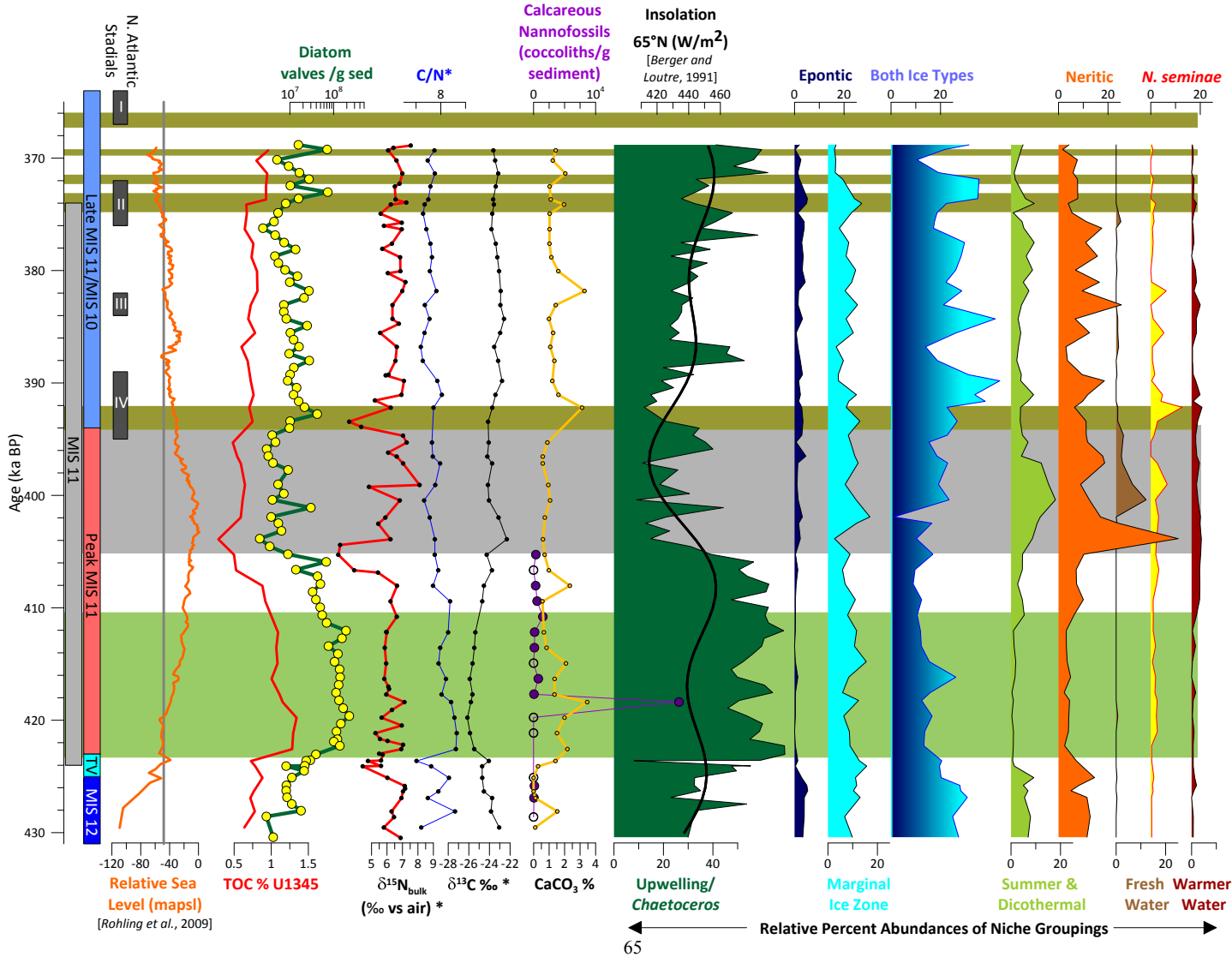

Clim. Past Discuss., doi:10.5194/cp-2015-184, 2016
Manuscript under review for journal Clim. Past
Published: 19 January 2016

Climate of the Past Discussions
Open Access
EGU

Figure 7. Summary of geochemistry and biological proxies. The grey vertical bar depicts the duration of MIS 11, colored vertical bars refer to the sections in the text, and dark grey bars show the timing of North Atlantic stadials (I-IV) (Voelker et al., 2010). Global eustatic sea level (orange) is plotted for reference. The sill depth of Bering Straight (-50 m apsl) is shown as a vertical grey line. Total organic carbon (red) is plotted with the total diatom abundance (green line, yellow dots). Geochemical data is plotted as $\delta^{15}N$ (red), C/N (blue), $\delta^{13}C$ (black), and % $CaCO_3$ (yellow). Biological proxies include absolute abundance of calcareous nannofossils (purple), and relative percent abundances of diatoms grouped by environmental niche (see color coding in Fig. 6). Insolation at 65° N (black) is overlain on *Chaetoceros* RS relative percent abundances. Type I Laminations are depicted as pale green bars and Type II laminations are depicted as olive green bars. A grey bar indicates the Beringian glacial advance.

Clim. Past Discuss., doi:10.5194/cp-2015-184, 2016
Manuscript under review for journal Clim. Past
Published: 19 January 2016

Climate of the Past Discussions
Open Access
EGU

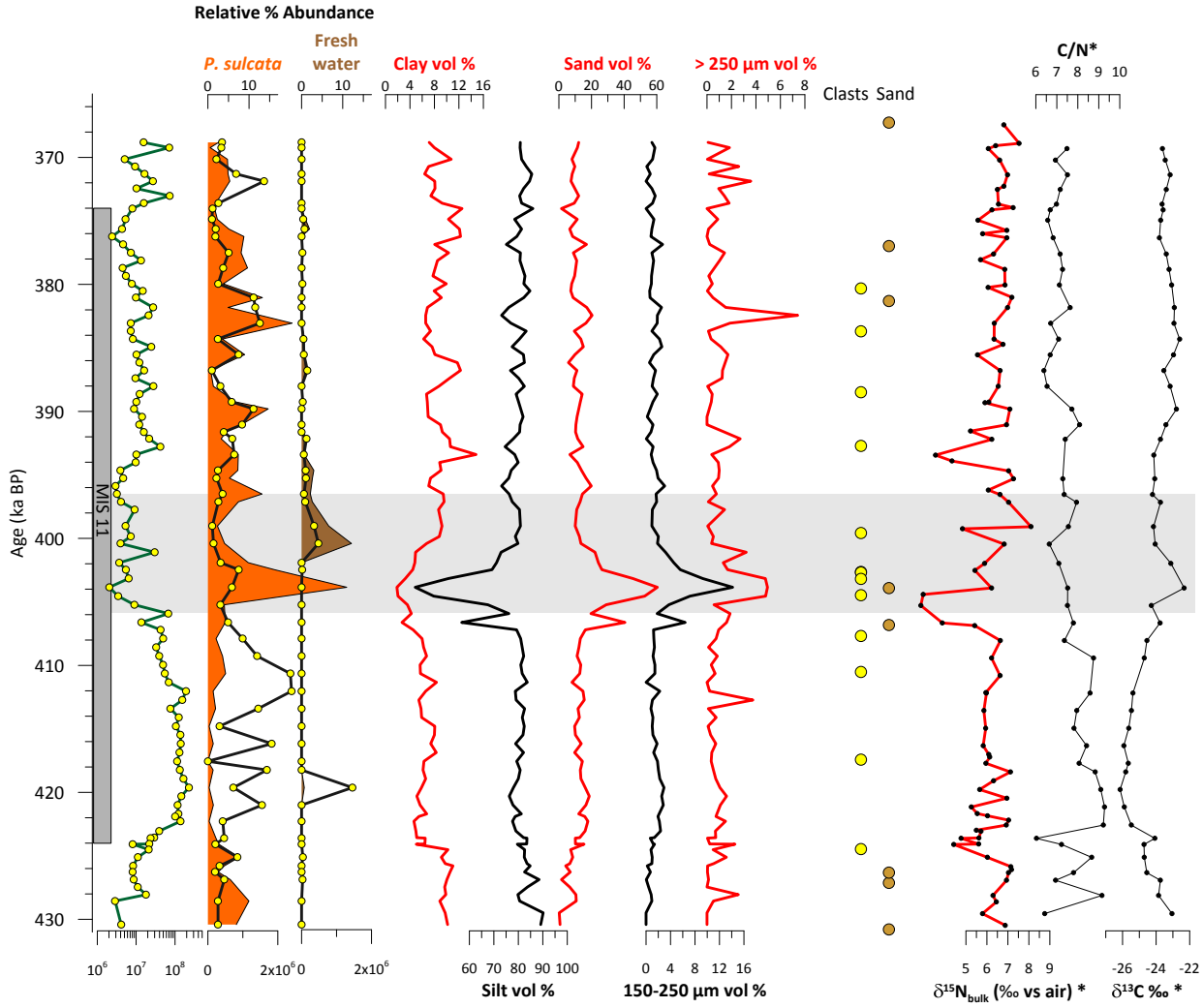

Clim. Past Discuss., doi:10.5194/cp-2015-184, 2016
Manuscript under review for journal Clim. Past
Published: 19 January 2016

Climate of the Past Discussions
Open Access
EGU

1469 Figure 8. Proxy indicators of shelf to basin transport. Total diatom absolute abundances
1470 are plotted next to absolute (line plots) and relative percent abundance of *P. sulcata*
1471 (orange area plot) and fresh water species (brown area plot). High-resolution grain size
1472 includes % clay, sand, and greater than 250 µm (red lines) and % silt and 150-250 µm
1473 (black lines). Yellow circles indicate isolated clasts (IRD), maroon circles indicate sand
1474 layers for all holes at U1345. Geochemical data is plotted as $\delta^{15}N$ (red), C/N (black), and
1475 $\delta^{13}C$ (black). The grey bar spans 406-396 ka, the interval of increased shelf to basin
1476 transport in Beringia.

1477